

Civil Engineering Support for the Traffic Monitoring Program

Final Report

Project No. BDV30-977-21

by

Ren Moses, Ph.D., P.E.
Department of Civil Engineering
FAMU-FSU College of Engineering
2525 Pottsdamer Street, Room 129
Tallahassee, FL 32310

September 2019

DISCLAIMER

The opinions, findings, and conclusions expressed in this publication are those of the authors and not necessarily those of the State of Florida Department of Transportation.

METRIC CONVERSION FACTORS

1 inch = 2.54 cm

1 mph = 1.609 km/h

1 pound = 0.4536 kg

Fahrenheit degrees = $9/5 \times$ Celsius + 32

1 kip = 4.4482216 kN

TECHNICAL REPORT DOCUMENTATION PAGE

1. Report No.	2. Government Accession No.	3. Recipient's Catalog No.	
4. Title and Subtitle Civil Engineering Support for the Traffic Monitoring Program		5. Report Date September 2019	
		6. Performing Organization Code	
7. Author(s) Ren Moses		8. Performing Organization Report No.	
9. Performing Organization Name and Address Department of Civil Engineering FAMU-FSU College of Engineering 2525 Pottsdamer Street, Room 129 Tallahassee, FL 32310		10. Work Unit No. (TRAIS)	
		11. Contract or Grant No. BDV30-977-21	
12. Sponsoring Agency Name and Address Florida Department of Transportation 605 Suwannee St. MS 30 Tallahassee, Florida 32399 (850) 414-4931		13. Type of Report and Period Covered Final Report October 2017 to September 2019	
		14. Sponsoring Agency Code	
15. Supplementary Notes Prepared in cooperation with the USDOT and FHWA			
16. Abstract Monitoring traffic through extensive collection and efficient storage of traffic data is crucial for improving safety and efficiency of Florida highways. To this end, the Florida Department of Transportation's Office of Transportation Data and Analytics operates temporary and permanent count stations strategically placed at various locations on the State Highway System. Consequently, the Office is faced with the continuing challenge of maintenance, sustainability, modernization of processes and equipment, and assurance of the quality of data collected from these sites. This project was aimed at providing civil engineering support for the operation of the traffic monitoring sites by undertaking four major tasks: (1) evaluation of products in the data collection chain; (2) evaluation of the quality of data; (3) evaluation of vehicle classification; and (4) evaluation of bike-ped detection systems. The report is divided into four chapters detailing the task undertaken, the results obtained, and the recommendations made. A number of recommendations have either been implemented or are under consideration for deployment with the purpose of improving the performance of the traffic monitoring sites.			
17. Key Word Traffic monitoring, weigh-in-motion, vehicle classification, bike-ped detection		18. Distribution Statement No restrictions	
19. Security Classif. (of this report) Unclassified	20. Security Classif. (of this page) Unclassified	21. No. of Pages 90	22. Price

Form DOT F 1700.7 (8_72)

ACKNOWLEDGEMENTS

The author wishes to acknowledge the support and assistance of Mr. Eric Griffin (Project Manager), Steve Bentz, Victor Johnson, and other FDOT Transportation Data and Analytics staff who provided valuable critique and guidance in the execution of the project. Special thanks also go to Daniel Fore, Jonathan Headings, and the entire Marlins Engineering team stationed at the FDOT Springhill Office for their help with data collection, analysis, and review of the project deliverables and reports.

TABLE OF CONTENTS

DISCLAIMER.....	ii
METRIC CONVERSION FACTORS.....	ii
TECHNICAL REPORT DOCUMENTATION PAGE.....	iii
ACKNOWLEDGEMENTS	iv
LIST OF TABLES	vii
LIST OF FIGURES	viii
TASK 1: EVALUATION OF WIM SENSORS AT SITE 9907	1
1.1 Purpose and Scope	1
1.2 Field Equipment Setup	1
1.3 Methodology	2
1.4 Data Preparation	2
1.5 Data Analysis	3
1.6 Task 1 Conclusions and Recommendations.....	7
TASK 2: EVALUATION OF DATA QUALITY.....	8
2.1. Purpose and Scope	8
2.2. Study Site	8
2.3. WIM Sensors	9
2.4. WIM Data Loggers.....	9
2.5. Research Design.....	10
2.6. Calibration and Validation.....	11
2.7. Field Calibration, Validation, and Test Runs.....	13
2.8. Comparative Analysis of Weight Differences.....	14
2.9. Comparative Analysis of Axle Spacing Differences.....	17
2.10. Task 2 Conclusions and Recommendations.....	21
TASK 3: EVALUATION OF VEHICLE CLASSIFICATION.....	22
3.1 Purpose and Scope	22
3.2 Review of the Current Florida Classification Scheme.....	22
3.3 Methodology	30
3.4 Evaluation of Springhill Road LPL Array Performance	31

3.5	Task 3 Conclusions and Recommendations	37
3.6	References	38
TASK 4: EVALUATION OF PED-BIKE MONITORING SYSTEMS		39
4.1	Purpose and Scope	39
4.2	Study Site	39
4.3	Ped-Bike Systems	40
4.4	Research Design	43
4.5	Data Extraction and Analysis	43
4.6	Task 4 Conclusions & Recommendations	48
APPENDIX A – CAT Scale Certification		50
APPENDIX B – Test Runs		52
APPENDIX C – Individual Truck Plots Vs. Speed (Phase 1)		57
APPENDIX D – Decision Trees		59
APPENDIX E – Equipment Certification Form		64
APPENDIX F – RidePod BT Bike Tube Counter by <i>MetroCount</i>		67
APPENDIX G – HI-TRAC OH-PED by <i>Q-Free</i>		71
APPENDIX H – Urban Post MULTI by <i>Eco-Counter</i>		74
APPENDIX I – HI-TRAC CMU by <i>Q-Free</i>		77

LIST OF TABLES

TABLE 1.1	Distribution of Vehicles by Class	3
TABLE 2.1	Calibration and Validation Runs.....	13
TABLE 2.2	Calibration and Validation Runs.....	13
TABLE 2.3	Descriptive Statistics of Weight Differences	16
TABLE 2.4	Test of Equality of Variance.....	16
TABLE 2.5	Test of Equality of Means of GVW Differences	17
TABLE 2.6	Descriptive Statistics Axle Spacing Data.....	19
TABLE 2.7	Test of Equality of Variance of Axle 1-2 Spacing Data.....	19
TABLE 2.8	Test of Equality of Means of Axle 1-2 Spacing Data.....	20
TABLE 2.9	Inferential Statistics for the Axle 1-2 Spacing	20
TABLE 3.1	Current Florida DOT Vehicle Classification Scheme.....	23
TABLE 3.2	Types of Classifiers at Traffic Monitoring Sites.....	23
TABLE 3.3	Classification Scheme Implemented on EMU3.....	24
TABLE 3.4	Classification Scheme Implemented on ADR 3000	25
TABLE 3.5	Classification Scheme Implemented on Phoenix 2	26
TABLE 3.6	Classification Scheme Implemented on iSINC	27
TABLE 3.7	Axle Spacing Threshold Differences.....	28
TABLE 3.8	Decision Tree Differences	29
TABLE 3.9	Vehicle A (9.04 ft) Test Runs.....	32
TABLE 3.10	Vehicle B (11.19 ft) Test Runs	33
TABLE 3.11	Summary Statistics for the Axle Spacing Readings	36
TABLE 3.12	Inferential Statistics for the Axle Spacing Readings.....	37
TABLE 4.1	Results of MetroCount Bicyclists Detection.....	44
TABLE 4.2	Results of EcoCounter Pedestrians and Bicyclists Detection	47

LIST OF FIGURES

Figure 1.1	Setup at Site 9907.....	1
Figure 1.2	Scatterplot of Temperature and Differences in Weight.....	2
Figure 1.3	Correlation Heat Map.....	3
Figure 1.4	Hourly Plots of the Difference in Weight vs. Temperature	4
Figure 1.5	Density of the Differences in Weight at Various Temperature Readings	5
Figure 1.6	Boxplots of Differences in Weight at 5°F Intervals	5
Figure 1.7	Median Values of Differences in Weight vs. Temperature at 5°F Interval.....	6
Figure 1.8	Plot of Differences in Weight at 5,000 Pounds Interval vs. Temperature.....	6
Figure 1.9	Temperature vs. Percent Difference in Weight	7
Figure 2.1	Setup of WIM Equipment at Site 9900.....	8
Figure 2.2	Study Design.....	10
Figure 2.3	Photo of the First Calibration Truck.....	12
Figure 2.4	Graphical Display of Weight Errors.....	14
Figure 2.5	Boxplot of GVW.....	15
Figure 2.6	Graphical Display of Axle 1-2 Spacing.....	18
Figure 2.7	Boxplot of Axle 1-2 Spacing Differences.....	18
Figure 3.1	The Vehicle Classification Structure	22
Figure 3.2	Florida Telemetered Traffic Monitoring Site	30
Figure 3.3	Experimental Traffic Monitoring Site on Springhill Road	31
Figure 3.4	Test Vehicles Used with Axle Spacing of (a) 9.04 ft and (b) 11.19 ft.....	32
Figure 3.5	Vehicle A Test Runs Plot.....	34
Figure 3.6	Vehicle B Test Runs Plot.....	35
Figure 3.7	Distribution of Errors in Axle Spacing.....	36
Figure 4.1	Setup of Data Collection Equipment at Site 9900.....	39
Figure 4.2	RidePod BT Bike Tube Counter	40
Figure 4.3	Field Setup of HI-TRAC OH-PED Counter	41
Figure 4.4	Urban Post MULTI counter	42
Figure 4.5	HI-TRAC CMU Setup.....	43
Figure 4.6	Various test scenarios.....	44
Figure 4.7	Performance Analysis of HI-TRAC OP-ED bike-ped system	45
Figure 4.8	Performance Analysis of HI-TRAC CMU bike-ped sensing system	48

TASK 1: EVALUATION OF WIM SENSORS AT SITE 9907

1.1 Purpose and Scope

WIM systems are susceptible to producing inaccurate weight data. Weight data errors may be attributed to (1) dynamic factors (e.g., vehicle speed, vehicle suspension system, and profile of the pavement), (2) equipment (e.g., weigh-in-motion sensor used), (3) how a data logger interprets the signal, (4) improper calibration resulting in discrepancy between static and weigh-in-motion (WIM) weights, and (5) environmental factors such as temperature. The purpose of Task 1 as narrated in the scope of services was to evaluate products in the data collection chain to determine the efficacy of the products used. To this end, the performances of Kistler Lineas sensor vis-à-vis Roadtrax BL Class 1 sensor were evaluated by determining the likely influence of temperature on the differences in weight readings reported by the two sensors installed at Site 9907. Seasonal variations of temperature were to be captured by a temperature probe installed at the site to record ground temperature as discussed in the following section.

1.2 Field Equipment Setup

Figure 1.1 shows the setup of the sensor arrays and field equipment at Site 9907. The outside lane in the northbound direction has the two WIM systems – Kistler Lineas and Roadtrax BL Class 1 – installed sequentially and polled by one roadside data recorder, i.e., TDC EMU3. The data from Kistler-Loop-Kistler array are labelled in the TDC EMU3 data logger as Lane 1 data while the data from Class 1 BL-Loop-Class 1 BL array are labelled as Lane 5 data. A temperature sensor is installed in the center of this outside lane to the depth of approximately 1 inch to record ground temperature. The temperature is recorded whenever a vehicle is sensed.

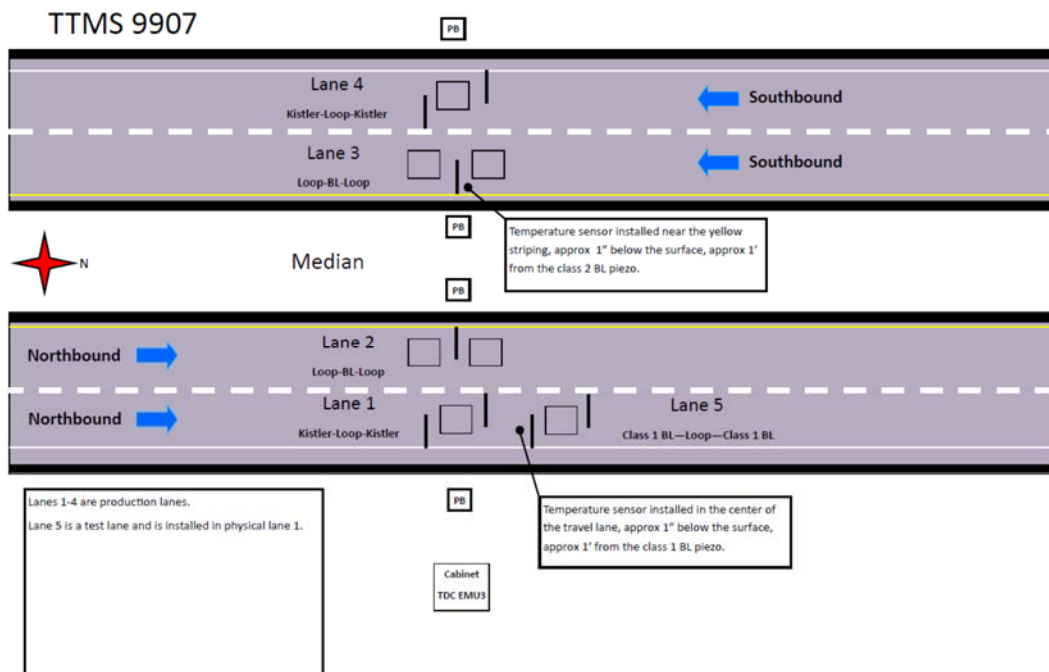


Figure 1.1 Setup at Site 9907

1.3 Methodology

A 3-step methodological process was adopted to determine the influence of ground temperature on the difference between the weights recorded by the two WIM sensors. The first step was the acquisition of per vehicle records of weight and temperature data from the two sensor arrays. The second step involved statistical analysis to assess the relationship between the differences in weight measurements by the two sensors and the recorded ground temperature. The third step was making conclusions and inferences from the information obtained through statistical analysis.

1.4 Data Preparation

The per vehicle records (PVR) were downloaded from the site's roadside data logger. The data files covered nine months, i.e., from May 2017 to January 2018. The collected data was first analyzed to find any missing temperature or weight readings or any anomalies in the data. There were no missing data during the analysis period; however, some anomalies in the data were discovered. The review of the data showed that on December 6, 2017 and again on December 11, 2017, the temperature sensor registered a temperature of -148 °F for approximate duration of 15 minutes. As the normal temperature registration was restored after 15 minutes, it was concluded that these two days had an abnormally low temperature recordings and were thus excluded from further analysis. In addition, outliers in the data were identified by plotting a scatterplot of temperature vs. differences in weight (Kistler minus BL) as shown in Figure 1.2. As can be deduced from Figure 1.2, the number of outliers is negligible as the distribution of the data is compact. The outliers were removed using a threshold value identified from the data observation.

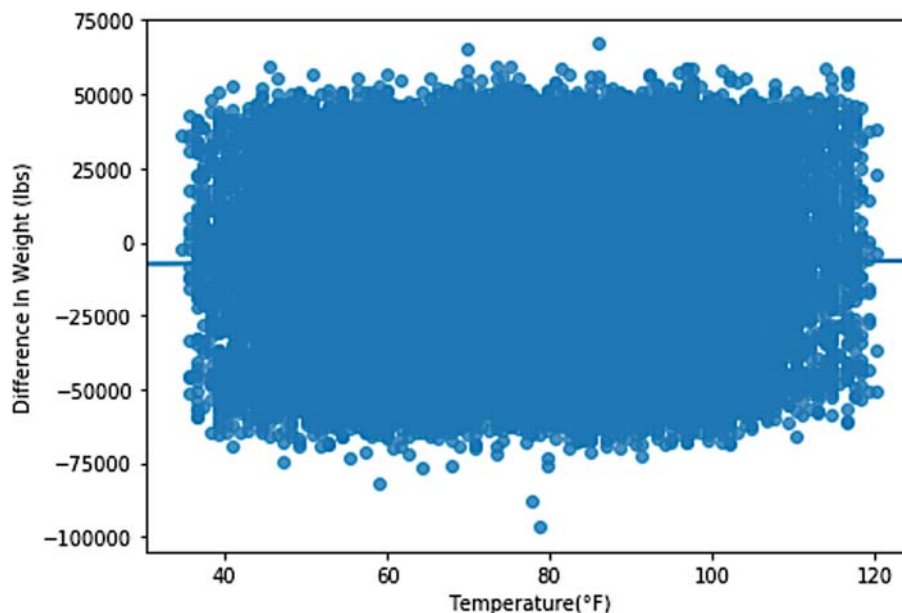


Figure 1.2 Scatterplot of Temperature and Differences in Weight

The analysis of vehicles by class during the period under review resulted in the distribution shown in Table 1.1. It is worth noting that lower class vehicles, i.e., Class 1 to Class 3 were omitted from

the dataset. Because of the prevalence of Class 9 vehicles and because the calibration of WIM sites generally utilizes Class 9 vehicles, it was decided that the analysis of the weight differences be focused on Class 9 trucks.

TABLE 1.1 Distribution of Vehicles by Class

Class	Number of Vehicles
Class 4	3491
Class 5	33,157
Class 6	10,441
Class 7	1,348
Class 8	20,928
Class 9	73,617
Class 10	903
Class 11	873
Class 12	947
Class 13	157

1.5 Data Analysis

After cleaning the data of outliers and other anomalies as explained above, statistical analysis was conducted to find the relationship between the recorded ground temperature and the difference in the weights calculated as follows:

$$\text{Percent Difference in Weight} = \frac{\text{Kistler} - \text{BL}}{\text{Kistler}} \times 100 \quad 1$$

in which all weights are in pounds. The differences in weight measurements were plotted against the temperature but due to a large number of mixed values there was no clear pattern. To this extent, a heat map was generated to determine the correlation between different variables. The heat map is shown in Figure 1.3. The results in Figure 1.3 shows that due to large variation of difference in weight values, the correlation between temperature and differences in weight is close to 0 suggesting that the correlation is insignificant.

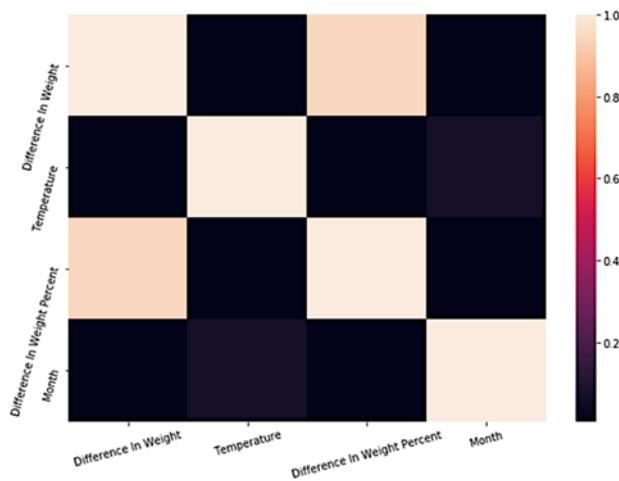


Figure 1.3 Correlation Heat Map

Further analysis of the data involved grouping the data based on the hour of occurrence. This was done with the purpose of determining if the variation of the difference in weight were correlated to the hour of recording. The results in Figure 1.4 show that the daily ground temperature peaked around 2:00 p.m. in the afternoon. The graph further shows a pattern of the difference in weight being maximum during the early hours of the day when the temperature is low, it drops as the temperature increases and then slightly increases again when the temperature starts decreasing. Even with this pattern, it is difficult to conclude that there is a correlation between the difference in weights and temperature. Similar analysis was conducted by grouping the data based on the month of occurrence. There were no monthly patterns observed between the difference in weight with respect to temperature.

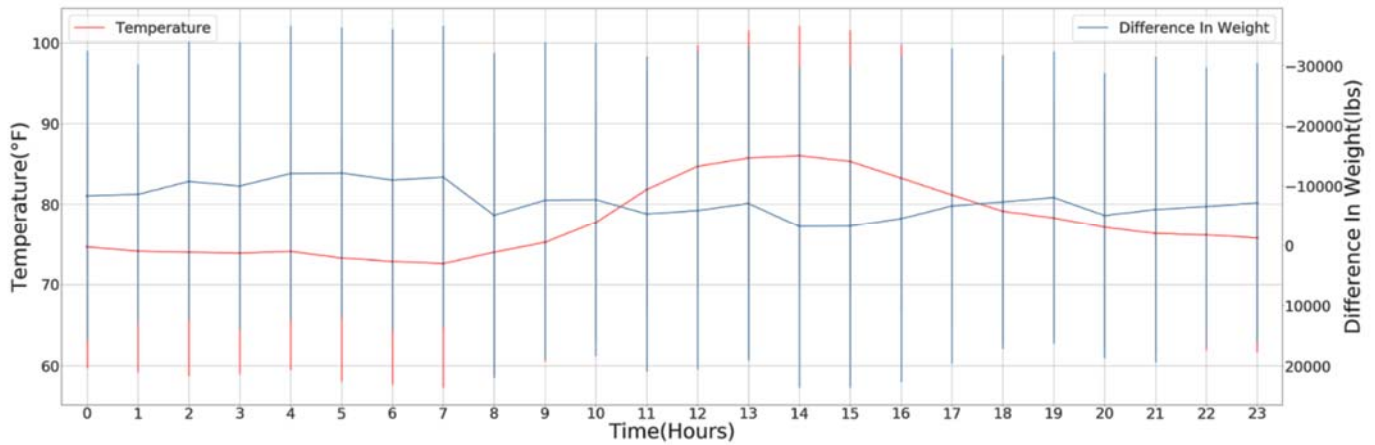


Figure 1.4 Hourly Plots of the Difference in Weight vs. Temperature

Due to the observed large variation in the distribution of difference in weight values, it was important to determine the density of data as it relates to the differences in weight. Joint plot was plotted to study the distribution. Figure 1.5 shows the data distribution of temperature and difference in weight. From Figure 1.5 it can be inferred that

- the readings are concentrated when the temperatures ranged from 60°F to 100°F,
- the distribution of difference in weight has three peaks, and
- the difference in weight can also take any value for the same temperature.

Using the results of the distribution graph shown in Figure 1.5 we divided the data into three parts based on the three peaks to find the relationship. Then these three parts of data were grouped into 5°F temperature interval and analyzed. No discernable pattern was revealed by this type of analysis.

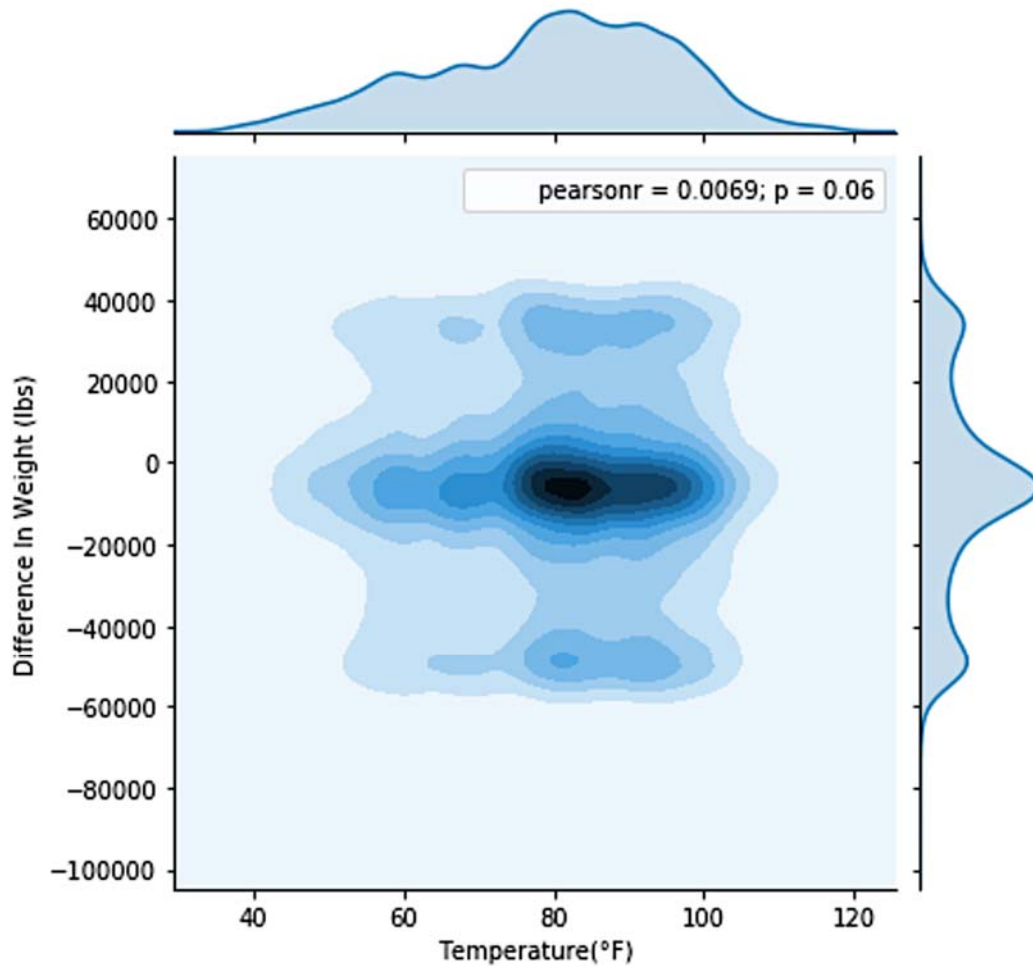


Figure 1.5 Density of the Differences in Weight at Various Temperature Readings

The boxplots in Figure 1.6 below show the variation of the differences in weight across all the recorded temperatures from low to high. The data are grouped based on 5°F temperature bins. As seen in Figure 1.6 the mean difference in weight remains almost the same for all the temperatures, but due to the presence of both positive and negative values, mean can mask the relationship and give incorrect results. Hence further analysis was conducted using the median values as discussed below.

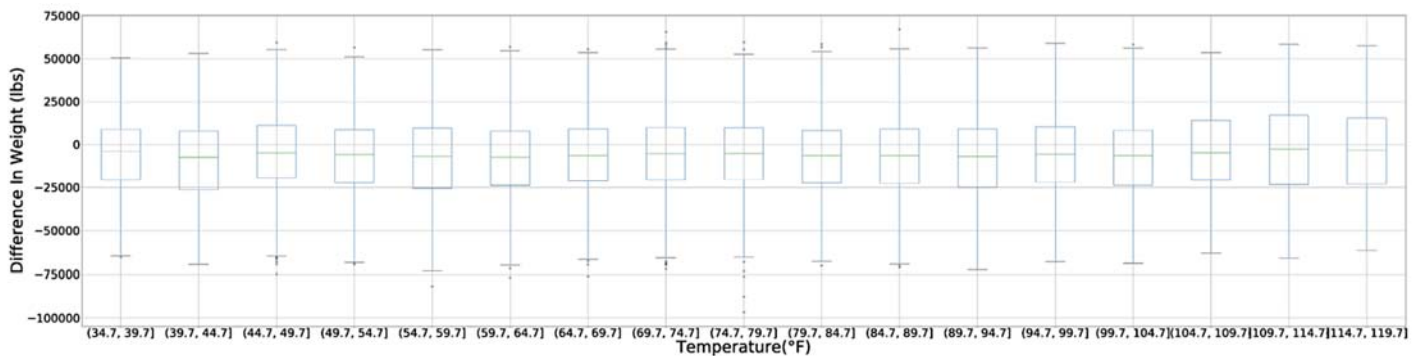


Figure 1.6 Boxplots of Differences in Weight at 5°F Intervals

Unlike Figure 1.6 data, Figure 1.7 shows the plot of the differences in weight using median values of weight differences. The median was calculated at 5°F intervals. Figure 1.7 does not show any clear pattern but we can see a sharp decrease in the differences in weight beyond 100 °F temperature recordings. Apart from that, the differences in weight varies in the range of 5,000 to 7,000 pounds.

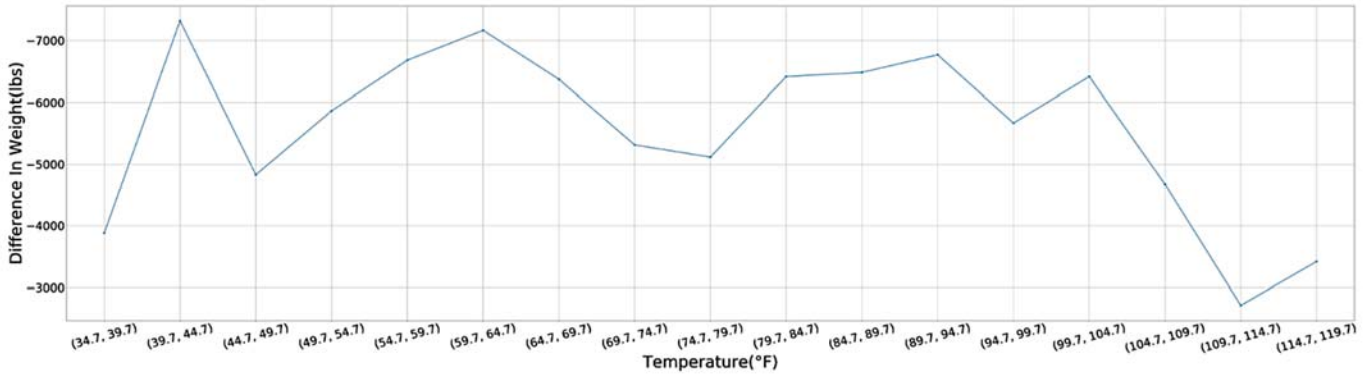


Figure 1.7 Median Values of Differences in Weight vs. Temperature at 5°F Interval

Further analysis were conducted by grouping the weight difference data at 5,000 pounds interval and plotting against the temperature. Figure 1.8 shows the variation of median temperature as the difference in weight increases. The median temperature is almost the same for all differences in weights. The temperature has a sudden spike when the differences in weight are very high.

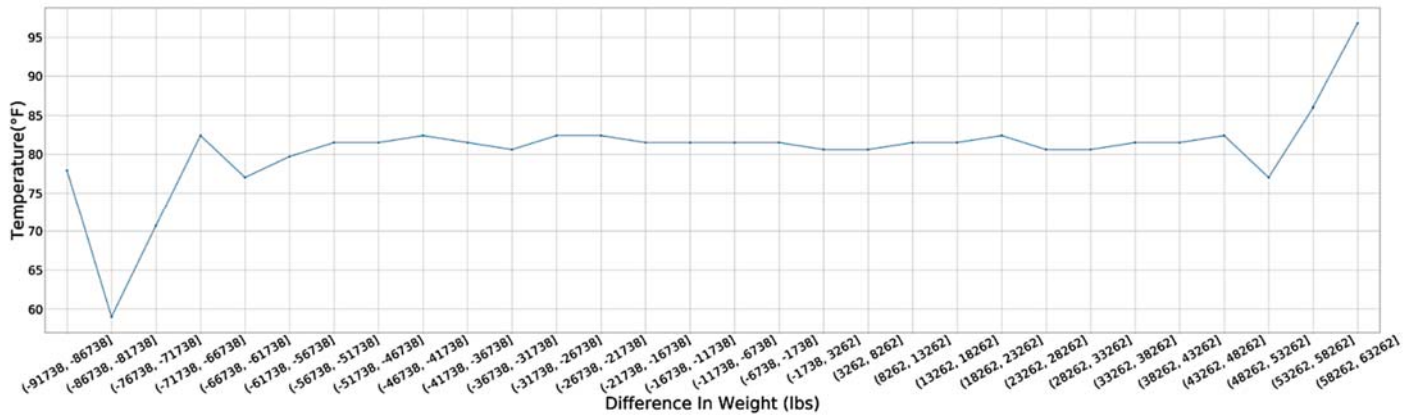


Figure 1.8 Plot of Differences in Weight at 5,000 Pounds Interval vs. Temperature

The differences in weight displayed in Figure 1.8 were converted into the differences in weight percent using Equation 1 shown earlier. In Figure 1.9, the percent difference in weight is plotted against temperature by calculating the median at every 50 percent differences in weight interval. The median temperature remains almost constant for difference in weights greater than -250 pounds, but it varies from 65°F to 95°F for difference in weights below that.

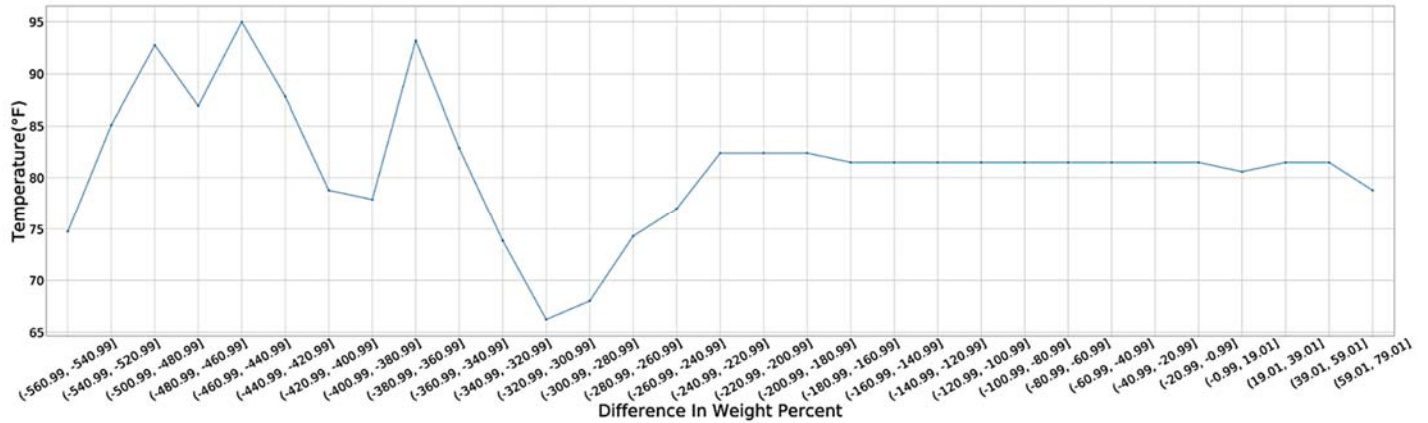


Figure 1.9 Temperature vs. Percent Difference in Weight

Similar analysis was conducted for all the classes of data, but the relationship between the differences in weight and temperature could not be inferred.

1.6 Task 1 Conclusions and Recommendations

This task was aimed at determining whether the difference in vehicle weights measured by two different sensors, i.e., Kistler Lineas and BL Class 1, are correlated with the ground temperature at the time of recording the weight values. The Kistler Lineas WIM sensor installed at Site 9907 uses weight measuring principle somewhat close to the BL Class 1 sensor. The Kistler Lineas WIM sensor operates in a way that when a force is applied to the sensor surface, the quartz elements yield an electrical charge signal proportional to the applied force. The BL Class 1 sensor uses piezoelectric material that detect a change in voltage caused by pressure exerted on the sensor by an axle and thereby measure the axle's weight.

It has been argued that fluctuation in ground temperature has an effect on ceramic and quartz material used in some WIM sensors. To this effect, data from Site 9907 where the two sensor types are installed back-to-back in the northbound outside lane were downloaded for a period of nine months. The analysis of the differences in vehicle weights show that although the differences were large, both in percent and absolute values, they had very little relationship with the recorded temperature.

There are a number of qualifications in this study, however. The study did not evaluate the effect of calibration and TNL curve adjustments that were undertaken during the analysis period. Although the dates of the events were known, calibration and adjustment parameters were not known. It is recommended that future calibration and TNL adjustment efforts should be well monitored and documented to determine their influence on weight measurements. In addition, lack of ground truth data, i.e., running a vehicle of know weight across both sensors, limited the scope of analysis to just determining the longitudinal differences in performance between Kistler and BL Class 1 sensor. Thus, if the cost of such undertaking permits, it is recommended that ground truth data be collected and used for comparative analysis purposes.

TASK 2: EVALUATION OF DATA QUALITY

2.1. Purpose and Scope

The quality of traffic data - both motorized and non-motorized – collected at traffic monitoring sites is influenced by various factors including technology used, installation and maintenance factors, environmental factors and data aggregation factors. In particular, the quality of weigh-in-motion (WIM) data is even more susceptible to not only these factors but to the quality of calibration and validation. The calibration and validation of WIM equipment require conducting numerous runs of a vehicle or vehicles of known parameters – axle spacings and weights – and adjusting calibration parameters to minimize the difference between static weights and dynamic weights being recorded by roadside WIM data loggers.

With the above background, the purpose of this task was to evaluate the accuracy of two WIM equipment – EMU3 WIM and iSINC WIM – by comparing the differences between recorded axle spacings and axle weights of vehicles with measured weights and measured dimensions. The test site on the Capital Circle Road, i.e., Site 9900, was chosen for conducting this study given that there are a number of sensor arrays on which various recorders can be hooked to. Efforts were made to ensure that the sensors were installed and were functioning properly prior to the commencement of calibration and validation processes. The following sections document study efforts and the results obtained.

2.2. Study Site

The testbed located at the Capital Circle Highway was utilized in this study. The testbed is designated as TTMS Site 9900 and was established in September 2014 for the purpose of consolidating field evaluations – that were scattered throughout the state – to one location; conducting short-term and long-term evaluation of piezos, loops, and sealants as well as conducting long term evaluation of WIM sensors. The testbed has also been equipped with the capability to evaluate intrusive and non-intrusive sensors and the accompanying data loggers. Figure 2.1 shows the setup of the test site.

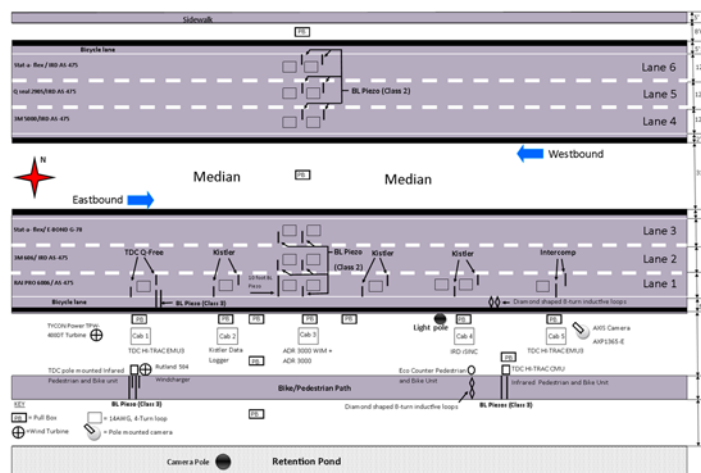


Figure 2.1 Setup of WIM Equipment at Site 9900

As can be seen in Figure 2.1, there are five WIM sensor arrays that can be utilized to evaluate WIM data loggers. The following sections discuss in sufficient detail the capabilities and limitations of data loggers and sensors.

2.3. WIM Sensors

The WIM data collection procedure starts with sensing of weights. The most common technologies for weighing vehicles are bending-plate systems, load-cell systems, and piezoelectric systems. A number of WIM sensors are installed at Site 9900, but two arrays with Kistler sensor shown in Figure 2.1 were utilized for this study. Lineas® WIM sensor, manufactured by Kistler, utilizes a quartz sensing system. The manufacturer's data sheet indicates that it can be installed in any kind of road pavement such as solid asphalt, drain asphalt, and concrete. The data sheet also states that in case of pavement rutting, the sensor's topcoat can be re-ground to match the profile of the road surface. The data sheet additionally claims that the performance of the Lineas® WIM sensors is not affected by changing weather conditions such as large variations of temperature, humidity, rain or sunshine.

2.4. WIM Data Loggers

All roadside data loggers for collecting WIM data generally have a similar principle of operation. They all require a power supply, loop card, WIM card, and communication unit installed in a small roadside cabinet. The following sections describe the two WIM data recorders that were evaluated at Site 9900.

2.4.1 EMU3 WIM data logger

The HI-TRAC® EMU3 by *Q-Free* data logger used for this study at Site 9900 is a 3rd generation data logger which includes 32 MB on-board Flash Memory and standard 8 GB Micro SD Memory which is expandable to 32 GB. The manufacturer's data sheet indicates that the unit incorporates interfaces to both piezoelectric sensors, inductive loop sensors, and a road installed temperature probe. The TDC HI-TRAC® EMU3 data logger can be powered from either main electric supply or solar panel and associated battery and charge regulator. The detection options include weigh-in-motion, axle classification, loop profiling classification, and cycle classification.

2.4.2 iSINC Data Logger

The iSINC® data logger forms the core of the International Road Dynamics Inc. traffic and truck Weigh-In-Motion (WIM) systems. The iSINC® roadside data logger interfaces with in-road sensors and camera but is also capable of connecting with communication systems and AVI readers. The iSINC unit used at Site 9900 has a quartz sensor module (KSM) for connecting with quartz WIM sensors. The KSM monitors, measures, and reports wheel or axle weight from multiple quartz sensors. It forwards road temperature data to the W3 (iSINC® WIM Control Unit) for use in temperature compensation. The data logger is capable of monitoring up to four quartz sensors simultaneously, reporting wheel or axle weights in real-time, forwarding road temperature data from an in-road temperature sensor, and producing real-time sensor signal traces on request.

2.5. Research Design

The main focus of this study was to evaluate the performance of EMU3 WIM and iSINC WIM data loggers in recording weights, axle spacings, and other vehicle parameters. Both systems were to be hooked up to Kistler WIM sensors installed on different arrays on the eastbound outside lane as shown in Figure 2.2.

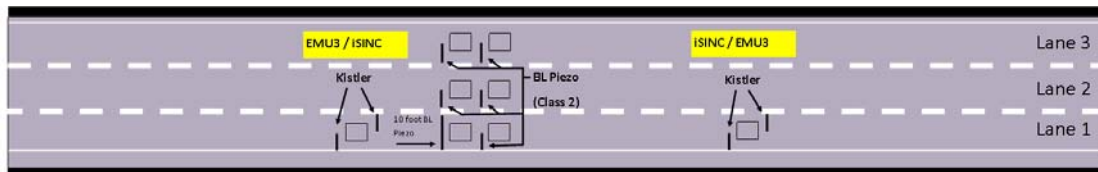


Figure 2.2 Study Design

To control for the effect of WIM sensor on data logging differences, the study was to be conducted in two phases. Phase 1 involved connecting EMU3 WIM data logger to the west array of sensors while connecting iSINC WIM data logger to the east array of sensors. In Phase 2, the data loggers were to be crossed in which the EMU3 WIM data logger is switched to the east array and iSINC WIM data logger is switched to the west array of sensors as shown in Figure 2.2.

Two Class 9 trucks owned by the Florida Department of Transportation were made available for this study. However, the study team decided that only one truck was to be utilized for calibration purposes because if two trucks were to make test runs, it would interfere with the calibration of iSINC since iSINC has quite a few parameters to be entered after each truck run. Based on the above details, the study was designed to proceed as follows:

- (a) Conduct advance inspection of the site equipment, sensors, cables, etc. to ensure that everything is working properly. Inspection also involved testing the signal strength of loops and WIM sensors to make sure that they fall within FDOT specifications.
- (b) Measure axle spacings and axle weights of the two trucks at the Midway Weigh Station and record the values.
- (c) On the first day of the study, connect EMU3 WIM data logger to the “west sensor array” and iSINC WIM data logger to the “east sensor array”. Label this as Phase I study.
- (d) Run the test truck (only one truck) at different speed points, preferably 30 MPH, 35 MPH, 40 MPH, 45 MPH, and 50 MPH while adjusting the calibration parameters to achieve a $\leq 5\%$ difference between recorded weights and static truck weight.
- (e) Conduct appropriate validation runs at each calibration speed point using two trucks.
- (f) Conduct additional runs at random speeds – ranging from low to high – to increase the sample size for comparative statistical analysis of the two data loggers. The target was a sample size of 30 runs (including validation runs in part (e)).
- (g) Switch EMU3 WIM data logger to the “east sensor array” and iSINC WIM data logger to the “west sensor array”. Label this as Phase II study.
- (h) Repeat parts (d) through (g).
- (i) Conduct various descriptive and inferential statistical analyses to evaluate the performance accuracy of EMU3 WIM and iSINC WIM in capturing weight and axle spacing data.

2.6. Calibration and Validation

WIM systems are susceptible to producing inaccurate weight data. Weight data errors may be attributed to (1) dynamic factors [e.g., vehicle speed, vehicle suspension system, and profile of pavement]; (2) equipment [e.g., WIM sensor used]; (3) how a data logger interprets the signal; and (4) improper calibration resulting in discrepancy between static and WIM weights. The purpose of calibration is generally to reduce WIM systematic errors. WIM calibration is performed by adjusting the sensitivity of the equipment to produce correct results – that is, axle weight and axle spacing values that are close to the ground truth values. Most WIM data loggers have one or more sensitivity or calibration factors that need to be adjusted as calibration runs are conducted. The following sections review calibration specifications and field observations of efforts to calibrate iSINC and EMU3 WIM data loggers.

2.6.1 EMU3 Calibration and Validation

According to the “HI-TRAC[®] Weigh-in-Motion Calibration Procedures and Temperature Compensation (TNL)” instruction manual dated July 2013, the operation of EMU3 relies heavily on proper setting of the so-called Temperature Non-Linearity (TNL) factors per degree centigrade per lane to correct for temperature variation of sensor output. Each WIM lane has a temperature compensation profile built up from the TNL factors. It is common for each lane in a system using the same sensors, resin and road surface type to have a different temperature compensation profile.

According to the manual, setting up the TNL factors and maintaining them is an important factor in ensuring the HI-TRAC WIM system is accurate. The manual enlists the correct process of setting up the Temperature Non Linearity Factors as follows:

1. Install sensors and HI-TRAC system.
2. Leave for a period (minimum 2 days but preferably 2 - 4 weeks) to collect data.
3. Determine TNL factors based on collected data (use a 6 Axle Truck front axle if sufficient vehicle records otherwise use a car, should be plenty of records – NB: they both give the same profile).
4. Calibrate the system noting the calibration temperature.
5. After 1 Month determine front axle weight per lane of 6 Axle Truck (or selected other vehicle type such as car) at temperature of calibration – this is the reference point or pivot value.
6. Adjust TNLs using this value as the pivot point and re-adjust on a regular basis (at least once every 2 months) until next calibration.

When calibrating the system, i.e., Step 4 above, the manual calls for applying the so-called Mean Impact Factor (MIF) to all the recorded axle weights. The impact factor (IF) for an axle is calculated as follows:

$$IF = \frac{\text{Mean of Recorded Weights (kg)}}{\text{Static Weight (kg)}}$$

The MIF is determined at the time of calibration. Normally calibration is performed with 3 vehicles of accurately measured axle weights. The vehicles are passed over each lane ten times. The Mean

Impact Factor (MIF) is determined by calculating the Impact Factor (IF) of each axle for the ten passes of the three vehicles. The mean of the impact factors determines the MIF.

2.6.2 *iSINC Calibration and Validation*

According to iSINC’s “Installation and Operations” manual dated April 20, 2010 the calibration of a WIM site with 2 axle sensors begins with calibrating axle spacings in which the software compares the calculated axle spacings to the actual axle spacings measured on the calibration truck and adjusts the axle spacing separation parameter in the software accordingly to reduce the error. Other parameters needing calibration are overall vehicle length, front of the vehicle to front axle distance, vehicle axle weights, and gross vehicle weight. The formula used to get a new calibration factor (CF) for gross vehicle weight (GVW) calibration is

$$\text{New CF} = \frac{\text{Actual GVW}}{\text{Average WIM GVW}} * \text{Current CF}$$

The average WIM GVW can come from one speed bin (i.e., range of speeds) but if data collected after the initial calibration indicate that weights are varying with speed, calibration factors for other speed ranges may be added to fine tune the system. The iSINC data logger also includes a “Dynamic Compensation” factor to ensure that front axle weights are also calibrated after calibrating GVW to the desired precision. Finally, once the initial weight calibration has been performed, autocalibration can be enabled if it is to be used.

2.6.3 *Calibration & Validation Trucks*

Two Class 9, Type 3S2 trucks, were provided by the Florida Department of Transportation. One of the trucks is shown in Figure 2.3. Each truck was weighed on a static scale at Midway Weigh Station as shown in the certifications that are attached in Appendix A.



Figure 2.3 Photo of the First Calibration Truck

The weights and measured axle spacing dimensions are shown in Table 2.1

TABLE 2.1 Calibration and Validation Runs

TRUCK #1							
ACTUAL WEIGHTS (pounds)				ACTUAL AXLE SPACINGS (feet)			
GVW	STEER AXLE	DRIVE AXLE	TRAILER AXLE	AXLE 1-2	AXLE 2-3	AXLE 3-4	AXLE 4-5
77,240	11,040	31,900	34,300	15.7	4.5	21.08	4.4
TRUCK #2							
ACTUAL WEIGHTS (pounds)				ACTUAL AXLE SPACINGS (feet)			
GVW	STEER AXLE	DRIVE AXLE	TRAILER AXLE	AXLE 1-2	AXLE 2-3	AXLE 3-4	AXLE 4-5
77,700	11,100	31,920	34,680	15.7	4.5	20.75	4.4

2.7. Field Calibration, Validation, and Test Runs

Following full inspection of study site, work on calibration for the first phase commenced in the morning of Tuesday, February 5, 2019. As indicated earlier, Phase 1 entailed EMU3 WIM data logger being connected to the West Kistler sensor “array” and iSINC WIM data logger being connected to the East Kistler sensor “array”. Also, as mentioned earlier the calibration runs were made with one truck only because of the quick turnaround times in relation to iSINC calibration. The number of runs made to achieve proper calibration and validation of the equipment for both Phase 1 and Phase 2 are shown in Table 2.2.

TABLE 2.2 Calibration and Validation Runs

Equipment	Total Calibration/Validation Runs					
	30 MPH	35 MPH	40 MPH	45 MPH	50 MPH	55 MPH
	PHASE 1 (EMU3 on West Array)					
EMU3 WIM	0/1	7/3	9/8	11/8	2/11	0/4
iSINC WIM	0/0	5/3	8/8	11/8	5/7	0/4
PHASE 2 (EMU3 on East Array)						
EMU3 WIM	0/0	0/9	0/21	5/18	0/18	0/3
iSINC WIM	0/0	7/2	7/8	8/7	6/11	0/3

The following issues were noted during the calibration, validation, and additional test runs:

- The difference in the number of calibration and validation runs recorded for each data logger (Table 2.1) is due to passes that were missed by the iSINC (as a result of communications error or operator error).
- EMU3 had fewer parameters to calibrate while iSINC had quite a number of parameters to calibrate as discussed earlier. Thus, iSINC calibration took longer.
- Once iSINC is switched to the calibration mode, one cannot access PVR data. Screen shots were taken to capture PVR. In EMU3, PVR data can be accessed during the calibration mode.

Figure 2.4 shows side by side comparison of the performance of the two data loggers when alternatively connected to the “east” and “west” sensor arrays. Visual examination of the graphs show that the calibration effort of both equipment at both sensor arrays (i.e., east and west) was able to achieve the accuracy level of within 5 percent of the static weight. There are possible outliers in the data [i.e., EMU3 Run 14 (Figure 2.4a) and iSINC Run 22 (Figure 2.4b)]. Appropriate statistical techniques will be used later to verify if these runs were indeed outliers. It is worth noting that the runs are sequential – meaning that the order increases with time.

Figure 2.5 shows the boxplots¹ of the difference between recorded GVW and actual GVW. The boxplots results mirrors the graphical results displayed earlier in Figure 2.4 in that EMU3 and iSINC performance were more different in Phase 1 (i.e., Figure 2.5a) than in Phase 2 (i.e., Figure 2.5b). Closer look at Figure 2.5 reveals that iSINC performance moved towards EMU3 performance in Phase 2 (i.e., Figure 2.5b).

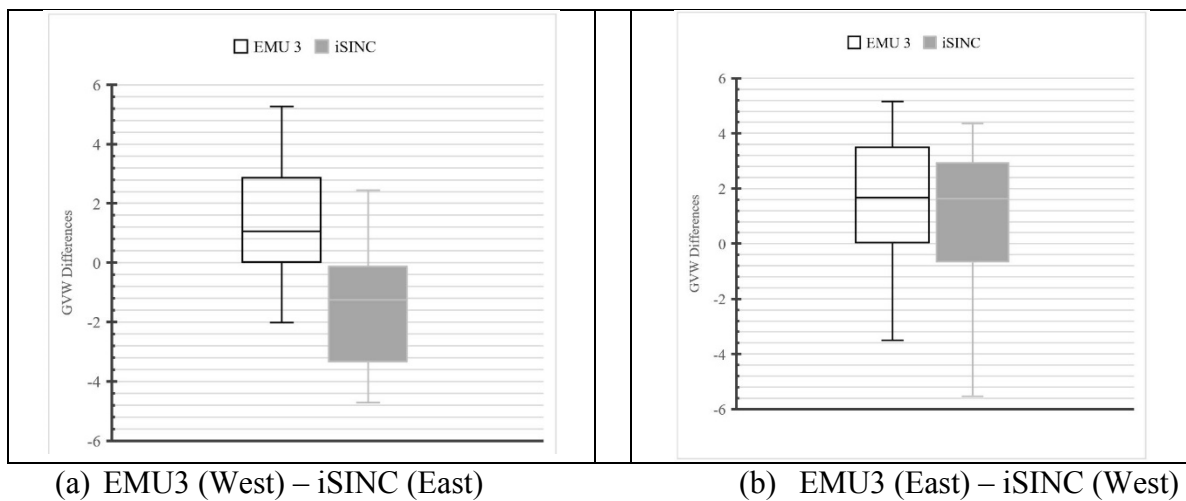


Figure 2.5 Boxplot of GVW

2.8.2 Descriptive Statistics of Gross Vehicle Weights

The Microsoft Excel and Matlab software were used to generate the relevant descriptive statistics of the gross vehicle weight differences between iSINC and EMU3 at both east and west sensor arrays. The descriptive statistics of the weight differences are shown in Table 2.3. The statistics displayed in Table 2.3 show that the mean %Difference for iSINC was -1.56% in Phase 1 of the study but turned positive, i.e., 1.03% in Phase 2 of the study. It is worth noting that EMU3 %Difference was positive (i.e., +1.35 and +1.56) in both Phase 1 and Phase 2 of the study. Another revelation in Table 2.3 is the very high coefficient of variation– the ratio of standard deviation to the mean (σ / \bar{x}).

¹ A boxplot (also known as a box-and-whisker diagram) is a convenient way of graphically depicting groups of numerical data through their [five-number summaries](#) (the smallest observation, lower [quartile](#) (Q1), [median](#) (Q2), upper [quartile](#) (Q3), and largest observation).

TABLE 2.3 Descriptive Statistics of Weight Differences

<i>EMU3 (West) - iSINC (East)</i>								
EMU3	30	+1.35	1.75	1.30	-2.01	5.27	0.19	-0.52
iSINC	30	-1.56	1.88	-1.20	-4.71	2.45	-0.07	-0.78
<i>EMU3 (East) - iSINC (West)</i>								
EMU3	31	1.56	2.19	1.40	-3.50	5.15	-0.37	-0.27
iSINC	31	1.03	2.35	2.28	-5.53	4.35	-0.91	0.54

Although both machines achieved the target accuracy of within 5 percent, however, the measurements were highly variable as shown by the very high coefficient of variation. The significance of the difference in the variability of data collection were tested using inferential statistical methods discussed below. In addition, the data seemed to be fairly symmetrical in Phase 1 and moderately skewed in Phase 2.

2.8.3 Inferential Statistics of Gross Vehicle Weights

There were two aspects of the study that required conducting statistical significance tests. First, we were interested in determining whether there was a significant difference between the EMU3 and iSINC performance on the first phase, i.e., EMU3 connected to the west sensor array while iSINC was connected to the east sensor array. Second, we were interested in determining whether there was a significant difference between the EMU3 and iSINC performance on the second phase, i.e., EMU3 connected to the east sensor array while iSINC was connected to the west sensor array. The results of a statistical significance analysis are reported below.

Test of the Equality of Variance

Statistical procedures required that prior to testing the significance of the difference between the averages of two sample data (i.e., EMU3 and iSINC), we first test the equality of variance between the two samples. Table 2.4 shows the results of equality of variance test.

TABLE 2.4 Test of Equality of Variance

Equipment	N	Lower	StDev	Upper	F-value	p-value
<i>EMU3 (West) - iSINC (East)</i>						
EMU3	29	0.41	1.75	1.82		
iSINC	29	0.55	1.88	2.43	1.1558	0.350
<i>EMU3 (East) - iSINC (West)</i>						
EMU3	30	0.42	2.19	1.80		
iSINC	30	0.56	2.35	2.39	1.1546	0.348

The results in Table 2.4 shows that for both Phase 1 [EMU3 (West) - iSINC (East)] and Phase 2 [EMU3 (East) - iSINC (West)], there is an overlap of EMU3 & iSINC in the 95% confidence

interval of the standard deviations, i.e., $P(Lower \leq \sigma \leq Upper)$. Both p -values are more than 95%, suggesting that we are more than 95 percent confident that the variances of both equipment in both phases were equal.

Test of the Equality of Means

We proceeded with analyzing the differences in the means using a statistical procedure that assumes equal variance. In this case, a paired t -test was chosen given that EMU3 and iSINC were measuring the weight of the same truck at each run. The results of the t -test are shown in Table 2.5. Judging by the p -values, the results in Table 2.5 show that the performance of EMU3 and iSINC were significantly different in Phase 1 (p -value = 0.000). However, in Phase 2, the performance of EMU3 and iSINC were not significantly different (p -value = 0.362). As indicated earlier, it is iSINC performance that changed in the two phases – i.e., moving closer to EMU3 performance in Phase 2.

TABLE 2.5 Test of Equality of Means of GVW Differences

Equipment	N	Mean	StDev	SE Mean
<i>EMU3 (West) - iSINC (East)</i>				
EMU3	58	1.35	1.75	0.3193899
iSINC	58	-1.56	1.88	0.343363
95% CI for mean difference: (-3.8476 , -1.9702)				
<i>t</i>-test for mean difference = 0 (Vs. not = 0): <i>t</i>-Value = -6.2032 <i>p</i>-Value = 0.000				
<i>EMU3 (East) - iSINC (West)</i>				
EMU3	60	1.56	2.19	0.3926
iSINC	60	1.03	2.35	0.4218
95% CI for mean difference: (-1.6824 , 0.6228)				
<i>t</i>-test for mean difference = 0 (Vs. not = 0): <i>t</i>-Value = -0.9194 <i>p</i>-Value = 0.362				

The EMU3 and iSINC 95 percent confidence intervals in Phase 1 were +0.69% to +2.00% and -2.27% to -0.86%, respectively. The EMU3 and iSINC 95 percent confidence interval in Phase 2 were +0.76% to +2.36% and +0.17% to +1.89%, respectively.

2.9. Comparative Analysis of Axle Spacing Differences

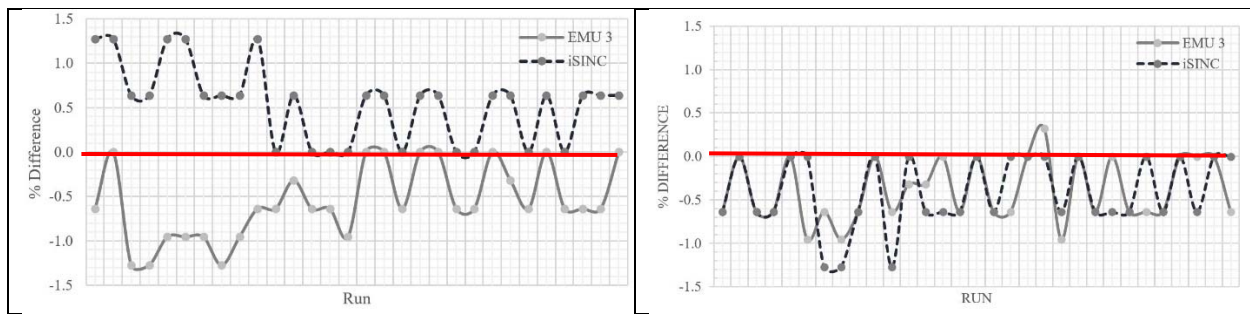
As for axle spacing, comparative analyses were conducted for Axle 1-2 and Axle 3-4 spacings. It was deemed that the spacing of tandem axles, i.e., Axle 2-3 and Axle 4-5 spacings, were too short – in the range of 4.5 to 4.6 feet – to reveal any appreciable difference in the performance of the two data loggers. The results discussed below are for Axle 1-2 spacings since the results of Axle 3-4 spacings mirrors those of Axle 1-2.

2.9.1 Graphical Overview of the Axle 1-2 Spacing Data

Figure 2.6 shows the graphical display of axle spacing recording errors. The % difference in axle spacing length was calculated as follows:

$$\% \text{Difference} = \frac{\text{Recorded Axle Length} - \text{Measured Axle Length}}{\text{Measured Axle Length}} \times 100\%$$

The data shown in Figure 2.6 is combined data for both Truck 1 and Truck 2. The separate plots for Truck 1 and Truck 2 showed that the error rate looks similar, thus the data can be combined for single analysis. In addition, the differences were plotted against speed. The plots showed that speed was not a major factor in the performance comparison. The curves in Figure 2.6, similar to weight analysis, again reveal that the performance of EMU3 and iSINC were different in Phase 1 but closer in Phase 2. In Phase 1 (Figure 2.6a), it can be seen that EMU3 data logger was consistently underreporting the lengths of Axle 1-2 and remained so even in Phase 2 (Figure 2.6b). However, iSINC was consistently overreporting the lengths in Phase 1 but underreported the lengths in a manner similar to EMU3 in Phase 2.

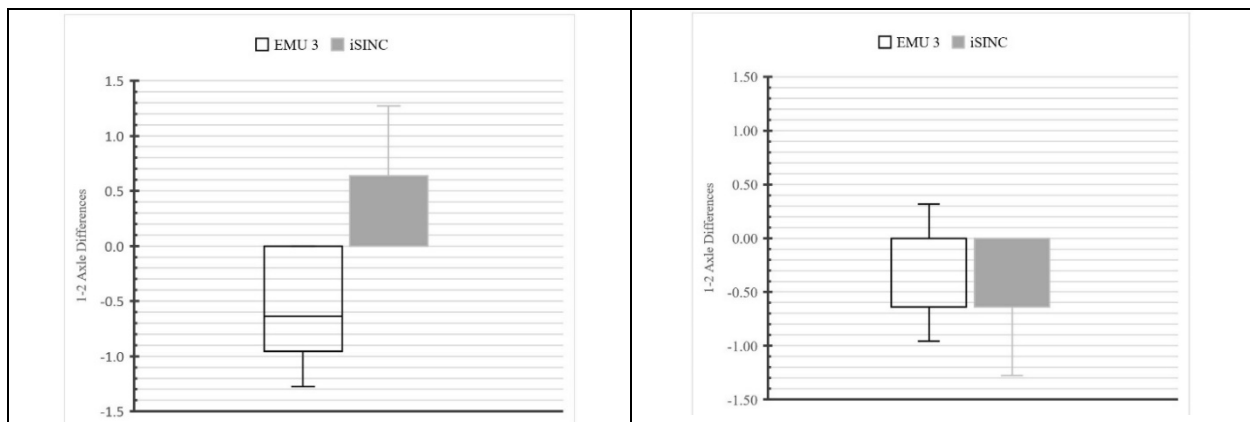


(b) EMU3 (West) – iSINC (East)

(b) EMU3 (East) – iSINC (West)

Figure 2.6 Graphical Display of Axle 1-2 Spacing

Figure 2.7 shows the boxplot of the difference between recorded Axle 1-2 lengths and measured Axle 1-2 spacing. The results in Figure 2.7 mirrors the results in Figure 2.6.



(a) EMU3 (West) – iSINC (East)

(b) EMU3 (East) – iSINC (West)

Figure 2.7 Boxplot of Axle 1-2 Spacing Differences

2.9.2 Descriptive Statistics of Axle 1-2 Spacing Measurements

The descriptive statistics of the recorded Axle 1-2 spacing data are shown in Table 2.5. The results in Table 2.6 shows that iSINC average %Difference was +0.55% in Phase 1 but changed to -0.41% in Phase 2 – which was closer to EMU3 average %Difference of -0.39%. The coefficient of variation of the axle spacing data is a bit lower than that of weight data analyzed in the previous section.

TABLE 2.6 Descriptive Statistics Axle Spacing Data

Equipment	Count	Mean	StDev	CoefVar	Minimum	Maximum	Skewness	Kurtosis
<i>EMU3 (West) - iSINC (East)</i>								
iSINC	30	0.55	0.43	0.79	0	1.27	0.17	-0.71
EMU3	30	-0.56	0.42	-0.74	-1.27	0	0.03	-0.92
<i>EMU3 (East) - iSINC (West)</i>								
EMU3	31	-0.39	0.37	-0.94	-0.96	0.32	0.19	-1.34
iSINC	31	-0.41	0.42	-1.02	-1.27	0	-0.53	-0.60

2.9.3 Inferential Statistics of Axle 1-2 Spacing Data

Inferential statistics were conducted to determine the significance of the difference in EMU 3 and iSINC performance in both Phase 1 and Phase 2. Again, the procedure starts by examining the equality of variances.

Test of the Equality of Variance of Axle 1-2 Spacing Data

Table 2.7 shows the results of equality of variance test. The results in Table 2.7 show that in both Phase 1 and Phase 2 there is an overlap in the 95% confidence interval of the standard deviation, i.e., $P(Lower \leq \sigma \leq Upper)$. Both p -values are high suggesting that we are more than 95 percent confident that the variances in both Phase 1 and 2 are equal.

TABLE 2.7 Test of Equality of Variance of Axle 1-2 Spacing Data

Equipment	N	Lower	StDev	Upper	F-Value	p-value
<i>EMU3 (West) - iSINC (East)</i>						
EMU3	29					
iSINC	29	0.52	0.43	2.29	1.091155	0.4079
<i>EMU3 (East) - iSINC (West)</i>						
EMU3	30					
iSINC	30	0.64	0.42	2.76	1.328696	0.22032

Test of the Equality of Means of Axle 1-2 Spacing Data

With the variances being equal as analyzed in Table 2.7, we can now proceed with the significance test of equality of means. The results are shown in Table 2.8.

TABLE 2.8 Test of Equality of Means of Axle 1-2 Spacing Data

Equipment	N	Mean	StDev	SE Mean
<i>EMU3 (West) - iSINC (East)</i>				
iSINC	58			0.079245
EMU3	58	-0.56	0.42	0.075863
<i>95% CI for mean difference: (0.8951 , 1.3342)</i>				
<i>t-test for mean difference = 0 (Vs. not = 0): t-Value = 10.1606 p-value = 0.000</i>				
<i>EMU3 (East) - iSINC (West)</i>				
EMU3	60	-0.39	0.37	0.065567
iSINC	60	-0.41	0.42	0.075586
<i>95% CI for mean difference: (-0.2207 , 0.1796)</i>				
<i>t-test for mean difference = 0 (Vs. not = 0): t-Value = -0.2053 p-value = 0.838</i>				

Again, a paired *t*-test was used for this purpose. The results in Table 2.8 confirm that EMU3 and iSINC average error in measuring Axle 1-2 spacing (0.55 ft vs. -0.56 ft) were significantly different in Phase 1 of the study. Similar to the weight analysis, iSINC performance crept closer to EMU performance resulting in the average error of -0.41 ft and -0.39 ft, respectively; which is statistically insignificant (*p*-value = 0.838). It was also of interest to evaluate how accurate was each data logger in capturing axle spacings. Table 2.9 shows the results of the “within equipment” variation in axle spacing readings.

TABLE 2.9 Inferential Statistics for the Axle 1-2 Spacing

Statistic	EMU 3 (West) / iSINC (East)		EMU 3 (East) / iSINC (West)	
	EMU3 (ft)	iSINC (ft)	EMU3 (ft)	iSINC (ft)
Error = Recorded – Actual Spacing	-0.09 ft	+0.09 ft	-0.06 ft	-0.06 ft
95% Confidence Interval	15.59 – 15.64 ft	15.76 – 15.81 ft	15.62 - 15.66 ft	15.61 – 15.66 ft
t-test	H ₀ : μ ₀ = 15.7 ft		H ₀ : μ ₀ = 15.7 ft	
	<i>t</i> _crit	±2.05 ft	±2.05 ft	±2.04 ft
	<i>t</i> _stat	-7.42 ft	+6.97 ft	-5.95 ft
	<i>p</i> -value	0.000	0.000	0.000

The efficiency of each equipment can be judged by assessing the 95 percent confidence interval of the resulting measurement errors. The results in Table 2.8 show that the 95 percent confidence

interval for EMU3 was below the true value, i.e., 15.7 ft, in Phase 1 and remained so in Phase 2. On the other hand, the 95 percent confidence interval of iSINC was above the true value but became lower than the true value in Phase 2.

2.10. Task 2 Conclusions and Recommendations

Calibration and validation of WIM equipment go a long way in improving the quality of WIM data. Consistent with this understanding, this research undertaking was aimed at evaluating the influence of calibration and validation on WIM data collected by two types of data loggers, i.e., EMU3 by Q-Free and iSINC by International Road Dynamics Inc. The equipment were installed at a test site, Site 9900, for evaluation purposes. Following a thorough inspection of sensors, cables, and other site equipment, calibration and validation were conducted over a 3-day period, i.e., February 5, 2019, through February 7, 2019. The research study took advantage of the availability of two Kistler sensor arrays at the site to test the effect of the sensors on data quality. This was achieved by conducting the study with EMU3 and iSINC connected on separate arrays in the first phase and then switching them around in the second phase. More than 30 validation and test runs were conducted in each phase using two calibration trucks.

The results indicate that the $\pm 5\%$ accuracy level in GVW capture was achieved as the 95 percent confidence level ranged from +0.69% to +2.00% and -2.27% to -0.86% for EMU3 and iSINC, respectively in Phase 1. In Phase 2, the 95 percent confidence intervals were +0.76% to +2.36% and +0.17% to +1.89% for EMU3 and iSINC, respectively. However, there were significant differences between EMU3 and iSINC in the first phase of the study. In the second phase of the study conducted the next day, there were no significant differences between EMU3 and iSINC in recording weights and axle spacings. This phenomenon can only be attributed to iSINC undergoing further improvement in calibration during the second phase of the study. There were a few issues worth mentioning that were observed in the course of the study,

- EMU3 had fewer parameters to calibrate while iSINC had quite a number of parameters to calibrate. Calibration of iSINC took more truck runs and time.
- Once iSINC is switched to the calibration mode, one cannot access PVR data. In EMU3, PVR data can be accessed during the calibration mode.
- iSINC reports left axle weight and right axle weight while EMU3 reports total axle weight.

The above results clearly show that the accuracy of ± 5 percent was achieved by both equipment, particularly in the second phase of the study. Based on the 95 percent confidence intervals of the percent errors (for both weight and axle spacing), it seems that even better accuracy can be achieved because the intervals were consistently above 0 or below 0 suggesting a systematic error that can be corrected by tweaking the calibration parameter(s). Further studies may be warranted to determine the sources of high variation in weight and axle spacing measurements that were observed. In addition, it is recommended that longitudinal studies should be conducted to determine if there are drifts in measurements and also to determine the degree of the drift.

TASK 3: EVALUATION OF VEHICLE CLASSIFICATION

3.1 Purpose and Scope

Changes in vehicle profiles and upgrades in roadside vehicle classifiers require continuous monitoring and evaluation of vehicle classification data. Previous work has shown that vehicle classification schemes might not be consistent across vendors. In addition, previous studies have shown a trend towards short cars and buses which lead to errors in classifying these vehicles, among others. The purpose of this task was to evaluate the performance of different classifiers in classifying vehicles. The evaluation was to be conducted first by examining the accuracy of axle spacing determination by different classifiers. Specifically, this study was aimed at accomplishing the following:

- comparing vehicle classification tables and decision trees used by different vendors' classification equipment,
- evaluating the existing vehicle classification table used by the Florida Department of Transportation,
- proposing an optimum vehicle classification table based on field data, and
- testing/validating the developed optimum classification table.

3.2 Review of the Current Florida Classification Scheme

The structure employed by the Florida Department of Transportation to classify vehicles into FHWA scheme is shown in the Figure 3.1 below. The input data for the classification task are generally the number of axles and axle spacing collected by roadway sensors. Axle weight is also used as an input wherever axle weight data are collected by weigh-in-motion sensors. The classification model is a descriptive model serving as an explanatory tool to distinguish vehicles of different classes. The output of the classification model is basically a target attribute of vehicles classes from Class 1 to Class 15 as defined in the FHWA F-Scheme, with Class 15 being a capture-all class for all unclassified vehicles.

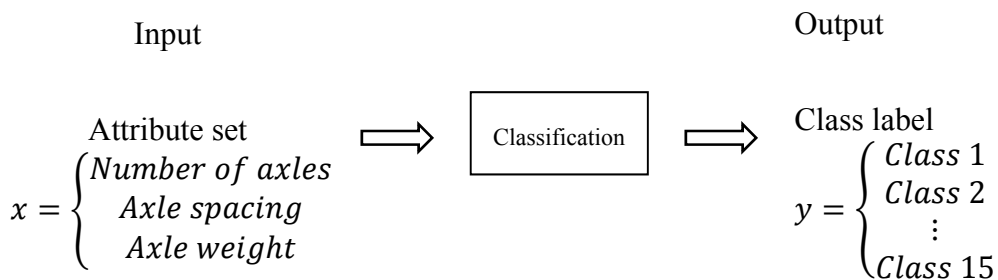


Figure 3.1 The Vehicle Classification Structure

The classification model can be a decision tree classifier, a rule-based classifier, neural networks, support vector machines, or naïve Bayes classifier. The FDOT system uses a decision tree classifier. The inclusion of axle weight as an attribute in vehicle classification tend to reduce errors as discussed later. However, the majority of sites in the Florida traffic monitoring program do not collect axle weight data, thus, classification relies on two attributes only – i.e., number of axles and axle spacing – as shown in Table 3.1 below.

TABLE 3.1 Current Florida DOT Vehicle Classification Scheme

Class	Axles	Axle Spacing (cm)							
		SP1	SP2	SP3	SP4	SP5	SP6	SP7	SP8
1	2	3 - 183							
2	2	183 - 305							
	3	183 - 305	183 - 762						
	4	183 - 305	183 - 762	3 - 183					
3	2	305 - 405							
	3	305 - 405	183 - 762						
	4	305 - 405	183 - 762	3 - 183					
	5	305 - 405	183 - 762	3 - 183	3 - 183				
4	2	701 - 1219							
	3	701 - 1219	3 - 183						
5	2	405 - 701							
	3	405 - 701	183 - 762						
	4	405 - 701	183 - 762	3 - 183					
	5	405 - 701	183 - 762	3 - 183	3 - 183				
6	3	183 - 701	3 - 183						
7	4	183 - 701	3 - 183	3 - 396					
8	3	183 - 701	335 - 1219						
	4	183 - 701	3 - 183	183 - 1341					
	4	183 - 701	335 - 1219	3 - 366					
9	5	183 - 792	3 - 183	183 - 1402	3 - 335				
	5	183 - 792	3 - 183	183 - 701	335 - 823				
10	6	183 - 792	3 - 183	3 - 1402	3 - 335	3 - 335			
	7	183 - 509	3 - 183	405 - 1219	3 - 405	3 - 405	3 - 405		
11	5	183 - 792	335 - 792	186 - 610	335 - 792				
12	6	183 - 792	3 - 183	335 - 792	183 - 732	335 - 792			
13	7	30 - 1372	30 - 1372	30 - 1372	30 - 1372	30 - 1372	30 - 1372		
	8	30 - 1372	30 - 1372	30 - 1372	30 - 1372	30 - 1372	30 - 1372	30 - 1372	
	9	30 - 1372	30 - 1372	30 - 1372	30 - 1372	30 - 1372	30 - 1372	30 - 1372	30 - 1372

The above table shows the current classification scheme used by the Florida Department of Transportation. This classification table is generally expected to be implemented by all vendors of classifiers installed at telemetered traffic monitoring sites in Florida. The scheme relies on two variables for classification, i.e., the number of axles each vehicle has and the spacing of those axles. The scheme is shown in metric units, i.e., in centimeters. A classifier output also depends on how different vendors implement the classification process. The review of installed equipment at all active Florida permanent classification sites showed the classifier distribution displayed in Table 3.1.

TABLE 3.2 Types of Classifiers at Traffic Monitoring Sites

Classifier	Vendor	Number of Sites
EMU3	Q-Free/TDC	29
ADR 3000	Peek Traffic	164
Phoenix 2	Diamond Traffic	64
EMU3 WIM	Q-Free/TDC	19
iSINC	IRD	19

In the following sections, the review of classification scheme implemented by various vendors, together with the associated decision trees are discussed.

3.2.1 EMU3 by Q-Free/TDC

Table 3.3 shows the classification scheme implemented by Q-Free/TDC on EMU3 classifiers utilized for classification at some Florida permanent count stations. The review of Table 3.3 shows that there are some differences between EMU3 table and the Florida classification table (i.e., Table 3.1) as narrated below:

- the minimum axle spacing is 10 cm as opposed to 3 cm in Table 3.1. Thus, vehicles with less than 10 cm axle spacing are probably thrown to Class 15.
- Table 2 does not have a 7-axle category in Class 13 while Table 3.1 has this category in Class 13.
- the SP1 axle spacing boundaries in Class 8 (3 and 4 axles) range from 305 to 701 cm in Table 3.2 while in Table 3.1 the range is 183 cm to 701 cm.

TABLE 3.3 Classification Scheme Implemented on EMU3

Class	Axles	Axle Spacing (cm)							
		SP1	SP2	SP3	SP4	SP5	SP6	SP7	SP8
1	2	10 - 183							
2	2	183 - 305							
	3	183 - 305	183 - 762						
	4	183 - 305	183 - 762	10 - 183					
3	2	305 - 405							
	3	305 - 405	183 - 762						
	4	305 - 405	183 - 762	10 - 183					
	5	305 - 405	183 - 762	10 - 183	10 - 183				
4	2	701 - 1219							
	3	701 - 1219	10 - 183						
5	2	405 - 701							
	3	405 - 701	183 - 762						
	4	405 - 701	183 - 762	10 - 183					
	5	405 - 701	183 - 762	10 - 183	10 - 183				
6	3	183 - 701	10 - 183						
7	4	183 - 701	10 - 183	10 - 183					
8	3	305 - 701	335 - 1219						
	4	305 - 701	335 - 1219	61 - 366					
	4	183 - 701	10 - 183	183 - 1341					
9	5	183 - 792	10 - 183	183 - 1402	10 - 335				
	5	183 - 792	10 - 183	183 - 701	335 - 823				
10	6	183 - 792	10 - 183	10 - 1402	10 - 335	10 - 335			
	7	183 - 509	10 - 183	405 - 1219	10 - 405	10 - 405	10 - 405		
11	5	183 - 792	335 - 792	183 - 610	335 - 792				
12	6	183 - 792	10 - 183	335 - 792	183 - 731	335 - 792			
13	8	10 - 1371	10 - 1371	10 - 1371	10 - 1371	10 - 1371	10 - 1371	10 - 1371	
	9	10 - 1371	10 - 1371	10 - 1371	10 - 1371	10 - 1371	10 - 1371	10 - 1371	10 - 1371
15	ALL OTHER VEHICLES								

The decision tree used by in EMU3 by Q-Free/TDC to classify vehicles is shown in Appendix D, Figure D1. The number of axles is determined first, followed by a check on the axles spacing. The

order of execution does not follow the sequence of operation. Given a number of axles, scanning through thresholds to determine the vehicle class does not follow the sequential order of classes. For example, for a 3-axle vehicle, the vehicle spacing is compared to available thresholds in the sequence of 8-4-6-3-2-5.

3.2.2 ADR 3000 by Peek Traffic

Table 3.4 shows the classification scheme implemented by Peek Traffic on ADR 3000. When compared with the FDOT classification scheme (shown in Table 3.1), some differences emerge as described below:

- Class 9 contains only one 5-axle group as opposed to two 5-axle groups in Table 3.1. In both tables the first two axles spacing (SP1 and SP2) are similar. The difference is observed in SP3 and SP4. The single 5-axle group in Table 3.4 spans from 183 cm to 1,402 cm for SP3 and 3 cm to 823 cm for SP4. In Table 3.1, the first 5-axle group has 183 cm to 1,402 cm and 3 cm to 335 cm as boundaries for SP3 and SP4, respectively. The second 5-axle group contains 183 cm to 701cm and 335 cm to 823 cm as boundaries for SP3 and SP4, respectively.

TABLE 3.4 Classification Scheme Implemented on ADR 3000

Class	Axles	Axle Spacing (cm)							
		SP1	SP2	SP3	SP4	SP5	SP6	SP7	SP8
1	2	3 - 183							
2	2	183 - 305							
	3	183 - 305	183 - 762						
3	4	183 - 305	183 - 762	3 - 183					
	2	305 - 405							
	3	305 - 405	183 - 762						
	4	305 - 405	183 - 762	3 - 183					
4	5	305 - 405	183 - 762	3 - 183	3 - 183				
	2	701 - 1219							
5	3	701 - 1219	3 - 183						
	2	405 - 701							
	3	405 - 701	183 - 762						
	4	405 - 701	183 - 762	3 - 183					
6	5	405 - 701	183 - 762	3 - 183	3 - 183				
	3	183 - 701	3 - 183						
7	4	183 - 701	3 - 183	3 - 183					
	3	305 - 701	335 - 1219						
	4	183 - 701	3 - 183	183 - 1341					
8	4	305 - 701	335 - 1219	61 - 366					
	5	183 - 793	3 - 183	183 - 1402	3 - 823				
9	6	183 - 793	3 - 183	183 - 1402	3 - 335	3 - 335			
	7	183 - 793	3 - 183	405 - 1219	3 - 405	3 - 405	3 - 405		
10	5	183 - 793	335 - 793	183 - 610	335 - 793				
11	6	183 - 793	3 - 183	335 - 793	183 - 732	335 - 793			
12	7	31 - 1372	31 - 1372	31 - 1372	31 - 1372	31 - 1372	31 - 1372		
	8	31 - 1372	31 - 1372	31 - 1372	31 - 1372	31 - 1372	31 - 1372	31 - 1372	
	9	31 - 1372	31 - 1372	31 - 1372	31 - 1372	31 - 1372	31 - 1372	31 - 1372	31 - 1372
13	ALL OTHER VEHICLES								

- the SP1 axle spacing boundaries in Class 8 (3 and 4 axles) range from 305 cm to 701 cm in Table 3.4 while in Table 3.1 the range is 183 cm to 701 cm.

The decision tree used in the ADR 3000 for classification is shown in Appendix D, Figure D2. The figure shows that the order of execution of the classification begins with the determination of the number of axles followed by the comparison of the axle spacing widths with the values in Table 3.4. The order of axles spacing check in this equipment is not the same as the order of classes. For example, for 2-axle vehicles, the order of execution is Class 3-2-1-4-5.

3.2.3 Phoenix 2 by Diamond Traffic

Table 3.5 displays the classification scheme implemented by Diamond Traffic on Phoenix 2 roadside data recorder. In addition to the numeral values for vehicle classes, some label names like cars, 2A-4T, buses, etc. are used to represent the vehicle classes. Table 3.5 shows these label names with equivalent class numbers in brackets. When compared with the FDOT classification scheme in Table 3.1, the following differences are observed:

TABLE 3.5 Classification Scheme Implemented on Phoenix 2

Class/Bin	Axles	Axle Spacing (cm)							
		SP1	SP2	SP3	SP4	SP5	SP6	SP7	SP8
Cycle (1)	2	3 - 183							
Cars (2)	2	183 - 305							
	3	183 - 305	183 - 762						
	4	183 - 305	183 - 762	3 - 183					
2A-4T (3)	2	305 - 405							
	3	305 - 405	183 - 762						
	4	305 - 405	183 - 762	3 - 183					
	5	305 - 405	183 - 762	3 - 183	3 - 183				
Buses (4)	2	701 - 1219							
	3	701 - 1219	3 - 183						
2A-SU (5)	2	405 - 701							
	3	405 - 701	183 - 762						
	4	405 - 701	183 - 762	3 - 183					
	5	405 - 701	183 - 762	3 - 183	3 - 183				
4A-ST (6)	3	183 - 701	3 - 183						
4A-SU (7)	4	183 - 701	3 - 183	3 - 183					
3A-SU (8)	3	305 - 701	335 - 1219						
	4	305 - 701	335 - 1219	61 - 366					
	4	183 - 701	3 - 183	183 - 1341					
5A-ST (9)	5	183 - 792	3 - 183	183 - 1402	3 - 335				
	5	183 - 792	3 - 183	183 - 701	335 - 823				
6A-ST (10)	6	183 - 792	3 - 183	3 - 1402	3 - 335	3 - 335			
	7	183 - 509	3 - 183	405 - 1219	3 - 405	3 - 405	3 - 405		
5A-MT (11)	5	183 - 792	335 - 792	183 - 610	335 - 792				
6A-MT (12)	6	183 - 792	3 - 183	335 - 792	183 - 732	335 - 792			
7+A-MT (13)	7	30 - 1372	30 - 1372	30 - 1372	30 - 1372	30 - 1372	30 - 1372		
	8	30 - 1372	30 - 1372	30 - 1372	30 - 1372	30 - 1372	30 - 1372	30 - 1372	
	9	30 - 1372	30 - 1372	30 - 1372	30 - 1372	30 - 1372	30 - 1372	30 - 1372	30 - 1372
Unused (14)	2	3 - 6							

- the SP1 axle spacing boundaries in Class 8 (3 and 4 axles) range from 305 cm to 701 cm in Table 3.4 while in Table 3.1 the range is 183 cm to 701 cm.
- Table 3.4 does not show Class 15 but it is assumed that all unclassified vehicles are thrown into Class 15. It is not clear what “Unused” in Class 14 mean.

The decision tree used by Phoenix 2 to classify vehicles is shown in Appendix D, Figure D3. The number of axles is determined first, followed by a check on the axles spacing. Similarly, depending on the number of axles, the order of execution may or may not follow the sequential order of classes (bins). For example, for a 2-axle vehicle, the execution follows the sequential order of bins 1-2-3-4-5 while in for 3-axle vehicles, the order used is 8-4-6-3-2-5.

3.2.4 iSINC by IRD

Table 3.6 shows the classification scheme implemented by IRD on iSINC classifier. Review of Table 3.6 shows some slight differences in boundary values in many classes. For example, the Class 8 (SP2) boundaries in Table 3.6 range from 335 cm to 1,222 cm while in Table 3.1 the range is from 335 cm to 1,219 cm.

TABLE 3.6 Classification Scheme Implemented on iSINC

Class	Axles	Axle Spacing (cm)									
		SP1	SP2	SP3	SP4	SP5	SP6	SP7	SP8	SP9	SP10
1	2	4 - 180									
	2	180 - 305									
2	3	183 - 305	183 - 762								
	4	183 - 305	183 - 762	3 - 183							
3	2	305 - 406									
	3	305 - 406	183 - 762								
	4	305 - 406	183 - 762	4 - 183							
	5	305 - 406	183 - 762	3 - 183	3 - 183						
4	2	702 - 1222									
	3	702 - 1222	4 - 183								
5	2	406 - 702									
	3	406 - 702	183 - 762								
	4	406 - 702	183 - 762	4 - 183							
	5	406 - 702	183 - 762	4 - 183	4 - 183						
6	3	183 - 702	4 - 183								
7	4	183 - 702	3 - 183	3 - 396							
8	3	305 - 702	335 - 1222								
	4	305 - 702	335 - 1222	61 - 366							
	4	183 - 702	4 - 183	183 - 1343							
9	5	183 - 792	4 - 183	183 - 1403	4 - 335						
	5	183 - 792	4 - 183	183 - 702	335 - 823						
10	6	183 - 792	4 - 183	4 - 1403	4 - 335	4 - 335					
	7	183 - 510	4 - 183	406 - 1219	4 - 406	4 - 406	4 - 406				
11	5	183 - 792	335 - 792	183 - 610	335 - 792						
12	6	183 - 792	4 - 183	335 - 792	183 - 732	335 - 792					
13	7	30 - 1372	30 - 1372	30 - 1372	30 - 1372	30 - 1372	30 - 1372				
	8	30 - 1372	30 - 1372	30 - 1372	30 - 1372	30 - 1372	30 - 1372	30 - 1372			
	9	30 - 1372	30 - 1372	30 - 1372	30 - 1372	30 - 1372	30 - 1372	30 - 1372	30 - 1372		
	10	30 - 1372	30 - 1372	30 - 1372	30 - 1372	30 - 1372	30 - 1372	30 - 1372	30 - 1372	30 - 1372	
	11	30 - 1372	30 - 1372	30 - 1372	30 - 1372	30 - 1372	30 - 1372	30 - 1372	30 - 1372	30 - 1372	30 - 1372

These differences appear to be due to conversion and approximation errors since the original table acquired from the vendor had its boundaries in feet with precision level of two decimal places.

This differs from the boundaries (in feet) in FDOT table which were presented as whole numbers. If the boundaries in the iSINC table are rounded to whole numbers before conversion, similar boundary values to Table 3.1 are obtained. Other differences observed between the two tables are as follows:

- the SP1 axle spacing boundaries in Class 8 (3 and 4 axles) range from 305 cm to 702 cm in Table 3.6 while in Table 3.1 the range is 183 cm to 702 cm.
- Class 13 contains 5 groups of axles spacing with 7, 8, 9 and 10 and 11 axles on Table 3.6 while the same Class 13 contains 3 groups of axles spacing with 7, 8 and 9 axles in Table 3.1. This difference implies that vehicles with 10 and 11 axles will be grouped into Class 13 if Table 3.6 is used, but thrown to Class 15 if Table 3.1 is used.

Appendix D, Figure D4 shows the decision tree used by iSINC classifier. Similar to other vendor's trees, the number of axles is determined first, followed by axle spacing. The order of execution in iSINC also does not follow the order of classes. For vehicles with 2 axles, for example, the order of execution is Class 2-3-4-5-1. The order of execution for other axles is shown in Figure D4 in Appendix D.

3.2.5 Review Summary of How Vendors Implement FDOT Classification Scheme

The previous sections have reviewed how each classifier implements the Florida classification scheme in terms of the required thresholds (i.e., axle spacing boundaries) and in terms of the decision tree. Table 3.7 summarizes five observed differences in thresholds.

TABLE 3.7 Axle Spacing Threshold Differences

	Diff. No.1	Diff. No. 2	Diff. No. 3	Diff. No. 4	Diff. No. 5
	Axles: 2 Class: 2 Spacing: SP1	Axles: 3 and 4 Class: 8 Spacing: SP1	Axles: 5 Class: 9 Spacing: SP3 and SP4	Axles: 7 Class: 13 Spacing: N/A	Axles: N/A Class: 13 Spacing: N/A
FDOT	3 – 183	183 – 701	1 st : SP3: 183 – 1402, SP4: 3 – 335 2 nd : SP3: 183 – 701, SP4: 335 – 823	Yes	7,8,9 axles
ADR 3000	3 - 183	305 – 701	SP3: 183 – 1402, SP4: 3 – 823	Yes	7,8,9 axles
EMU3	10 – 183	305 – 701	1 st : SP3: 183 – 1402, SP4: 3 – 335 2 nd : SP3: 183 – 701, SP4: 335 – 823	Yes	7,8,9 axles
Phoenix 2	3 - 183	305 – 701	1 st : SP3: 183 – 1402, SP4: 3 – 335 2 nd : SP3: 183 – 701, SP4: 335 – 823	Yes	7,8,9 axles
iSINC	4 - 183	305 – 702	1 st : SP3: 183 – 1403, SP4: 3 – 335 2 nd : SP3: 183 – 702, SP4: 335 – 823	Yes	7,8,9,10,11 axles

The first column of differences in Table 3.7 shows that for 2-axles spacing in Class 2, the lower threshold value for EMU3 is 10 cm while that of FDOT and other vendors is 3 cm. TDC responded that this difference in EMU3 is caused by the fact that the equipment cannot accept axle spacing inputs of less than 10 cm. The second column shows that, Class 8 vehicles with 3 and 4 axles, the lower boundaries of the FDOT scheme is 183 cm while for the rest of the vendors is 305 cm. The third column of differences shows how ADR 3000 table contains just a single range of threshold values for Class 9 vehicles with 5 axles. On the other hand, the FDOT table, as well as tables by other vendors, has two ranges of threshold values. The use of two ranges by other vendors exclude the vehicles with axle spacing 701- 1,402 cm for SP3 and 335 – 823 cm for SP4 to be included into a Class 5. The single range in ADR 3000 includes this type. Column 4 shows that EMU3 table does not have thresholds for 7-axle vehicles in Class 13. The last column of differences shows that, iSINC equipment will classify vehicles with 10 and 11 axles as Class 13 while other equipment will classify these vehicles as Class 15.

Another aspect in the comparative analysis of classifiers is the order of classification (decision tree). Table 3.8 summarizes the differences in vehicle classification sequences implemented by different vendors after the number of axles for a given vehicle is checked.

TABLE 3.8 Decision Tree Differences

Vendor	Order of execution (Classes)						
	2-axle	3-axle	4-axle	5-axle	6-axle	7-axle	8+
FDOT							
ADR 3000	3-2-1-5-4	3-6-8-2-5-4	7-8-8-2-5	9-3-11-5	10-12	10-13	N/A
EMU3*	2-3-4-5-1	8-4-6-3-2-5	8-8-7-3-5-2	9-9-11-3-5	10-12	10-13	N/A
Phoenix 2	1-2-3-4-5	8-4-6-3-2-5	8-8-7-3-5-2	9-9-11-3-5	10-12	10-13	N/A
iSINC	2-3-4-5-1	8-4-6-3-2-5	8-8-7-3-5-2	9-9-11-3-5	10-12	10-13	N/A

*The EMU3 decision tree shown is at Site 32-0112 on Interstate 75. The vendor indicated that the decision tree can be changed per client’s requirements.

The review of literature shows that decision tree has an effect in classification accuracy (Masaki, 2016; Refai et al, 2014). Due to overlap of axle spacing among classes, a vehicle with the same number of axles can fall into two or more classes. Thus, which class is checked first has consequences. A recent study in Florida (Masaki, 2016) revealed that the percentage of misclassified Class 4 vehicles dropped by 3% when the order of classification for 2-axles vehicles changed from 1→3→2→4→5 to 1→3→2→5→4. The differences in the classification trees used by different vendors may suggest that Florida DOT may need to provide guidelines on decision tree implementation.

3.2.6 FDOT Guidelines on Traffic Monitoring Equipment

The FDOT Traffic Monitoring Handbook (FDOT, 2018) provides guidelines for certification of traffic monitoring equipment (see Appendix E). The guidelines require that each portable traffic volume and classification counters used by the department or consultants for general data collection activities of other Department projects be certified for accuracy once each year. A

minimum of 15-minute count is required. For vehicle classification counters, two conditions must be met: First, the total volume counted by the equipment should be within 10% of the ground truth volume. Second, the classified volumes are grouped into four main groups: (a) Classes 1 through 3, (b) Classes 4 through 8, (c) Classes 9 through 13, and (d) Class 15. The total volume for each group should be within 10% of the corresponding volumes of the ground truth data. It is not clear if the broad nature of these guidelines has led to different vendors implementing different decision trees and possibly different thresholds as discussed earlier.

3.3 Methodology

The Transportation Data and Analytics Office of the Florida Department of Transportation (FDOT) maintains more than 275 roadway traffic monitoring sites on the Florida State Highway System. Over 240 sites are classification sites while 35 sites are weigh-in-motion (WIM) sites capable of capturing vehicle weight as well as the number of axles and axle spacings. Traffic monitoring sites can be telemetered or portable. Telemetered sites are composed of sensors installed on the roadway, a power supply system, a cellular modem, and a computer cabinet. Portable traffic monitoring sites are similar to telemetered traffic monitoring sites except that they don't have a cellular modem or any power supply system. Figure 3.2 shows an example of a telemetered traffic monitoring site.



Figure 3.2 Florida Telemetered Traffic Monitoring Site

This study was aimed at evaluating the accuracy of classification at classification sites only. Classification at WIM sites involves the use of vehicle weights in the classification process. The WIM sites are frequently calibrated to ensure proper weight measurements. A separate study that involves evaluating of the quality of WIM data was planned and accuracy of classification at WIM sites will be evaluated in the process.

A number of criteria was used in selecting study sites, including geographical location, roadway functional classification, urban vs. rural, and the distribution of vehicles at the study site. The ground truth data were to be collected at the vicinity of the selected sites using a video camera.

Synchronization of the video camera time with the system time in the automatic data recorders was to be done prior to data collection to enable vehicle matching during data processing. Individual vehicle records for the time when the video was logged on were to be downloaded from the computers installed at the classification sites using polling software and modem connection. The ground truth data were to be compared with machine classification to identify errors in vehicle classification. Classification using ground truth data was to follow the guidelines provided in the existing Florida classification table that was earlier displayed in Table 3.1.

3.4 Evaluation of Springhill Road LPL Array Performance

Prior to embarking on full-fledged data collection at various TTMS sites around the state, it was decided that the set-up at the Springhill Road evaluation site be utilized to test the performance of classifiers in interpreting loop and piezo data. This site has two Loop-Piezo-Loop (LPL) arrays installed back to back on the southbound lane. Each array can be connected to a separate classifier resident in the FDOT office nearby. The purpose of this evaluation was to determine how two classifiers report axle spacing lengths of vehicles of known axle length dimensions. Figure 3.3 shows the Springhill Road test site.



Figure 3.3 Experimental Traffic Monitoring Site on Springhill Road

3.4.1 Data Collection

Two test vehicles with known axle spacing were used to perform a number of test runs at this site for the purpose of comparing ground truth axle spacing to machine-reported axle spacing. Both vehicles were vans with axles spacing of 9.04 feet and 11.19 feet. The vehicle profiles are shown in Figure 3.4. Two classifiers were used in this experiment, i.e., EMU3 and ADR 3000. The classifiers were hooked up to different LPL array at the site. It was not deemed important at this stage of the experiment to cross the hook ups to control for LPL array differences.



Figure 3.4 Test Vehicles Used with Axle Spacing of (a) 9.04 ft and (b) 11.19 ft

Following calibration of the spacing parameter in the classifiers, a total of 29 test runs were made with Vehicle A and 30 test runs with Vehicle B. The test runs were conducted on Thursday, October 4th, 2018 and on Thursday, October 23rd, 2018 in the morning hours. Table 3.9 shows the axle spacing measurements as reported by EMU3 and ADR 3000 for the 29 trial runs for Vehicle A with a ground truth axle length of 9.04 feet. Vehicle A was driven at random speeds ranging from 30 mph to 50 mph to determine if speed has an effect on axle spacing measurements. The speeds reported by EMU3 and ADR 3000 are also shown in Table 3.9.

TABLE 3.9 Vehicle A (9.04 ft) Test Runs

Run #	Ground Truth Axle Spacing (ft)	Machine Reported Axle Spacing (ft)		Machine Reported Speed (mph)	
		EMU3	ADR 3000	EMU3	ADR 3000
1	9.04	8.73	8.65	20	17
2	9.04	8.99	9.28	36	36
3	9.04	9.25	8.83	40	37
4	9.04	8.99	8.91	38	38
5	9.04	9.45	9.13	29	30
6	9.04	9.12	8.84	32	31
7	9.04	8.99	8.93	33	32
8	9.04	9.22	8.78	36	33
9	9.04	9.15	8.75	35	32
10	9.04	8.76	8.92	40	40
11	9.04	8.86	8.98	38	37
12	9.04	9.15	8.72	41	38
13	9.04	8.69	10.19	47	50
14	9.04	9.15	8.78	37	34
15	9.04	9.06	8.68	48	45
16	9.04	8.89	8.46	38	35
17	9.04	9.02	8.55	32	30
18	9.04	8.96	8.94	42	41
19	9.04	9.19	9.15	42	42
20	9.04	8.92	8.84	38	37
21	9.04	9.06	8.84	42	40
22	9.04	9.15	8.65	36	34

TABLE 3.9, continued

Run #	Ground Truth Axle Spacing (ft)	Machine Reported Axle Spacing (ft)		Machine Reported Speed (mph)	
		EMU3	ADR 3000	EMU3	ADR 3000
23	9.04	8.99	8.83	38	36
24	9.04	9.22	9.02	41	40
25	9.04	9.06	8.78	40	38
26	9.04	9.09	8.67	43	41
27	9.04	9.12	8.83	36	31
28	9.04	9.09	9.14	38	37
29	9.04	9.12	8.73	31	30

The results in Table 3.9 shows that the machine-reported axles spacing range from 8.69 feet to 9.45 feet for EMU3 and 8.46 feet to 10.19 feet for the ADR 3000. Closer look at EMU3 reported axle spacing reveals that 14 out of 29 records fall above the ground truth axle spacing of 9.04 feet while in the ADR 3000 results only 5 out of 29 records fall above the ground truth value.

Table 3.10 shows the results of the test runs for Vehicle B with 11.19 feet axle spacing. Test runs for Vehicle B were made with a target speed ranging from 30 mph to 50 mph with increment of 5 mph. The target speeds, reported axle spacings, and reported speeds are all shown in Table 3.10.

TABLE 3.10 Vehicle B (11.19 ft) Test Runs

Run #	Ground Truth Axle Spacing (ft)	Machine Reported Axle Spacing (ft)		Target Speed (mph)	Machine Reported Speed (mph)	
		EMU3	ADR 3000		EMU3	ADR 3000
1	11.19	11.29	11.72	30	29	30
2	11.19	11.48	11.47	35	34	34
3	11.19	11.09	11.21	40	39	39
4	11.19	11.71	10.10	40	40	41
5	11.19	11.38	11.81	50	50	53
6	11.19	11.65	11.38	30	31	30
7	11.19	11.55	11.74	35	36	36
8	11.19	11.75	11.67	40	41	41
9	11.19	10.96	12.22	45	43	48
10	11.19	11.75	11.51	50	51	49
11	11.19	10.96	11.15	30	30	30
12	11.19	11.48	11.10	35	35	33
13	11.19	11.09	11.11	40	38	38
14	11.19	11.25	11.29	45	43	42
15	11.19	11.38	11.42	50	50	50
16	11.19	11.02	11.00	30	30	29
17	11.19	10.99	11.47	35	34	35
18	11.19	11.38	10.94	40	40	38
19	11.19	11.29	11.09	45	45	44
20	11.19	11.25	11.51	50	49	50

TABLE 3.10, continued

Run #	Ground Truth Axle Spacing (ft)	Machine Reported Axle Spacing (ft)		Target Speed (mph)	Machine Reported Speed (mph)	
		EMU3	ADR 3000		EMU3	ADR 3000
21	11.19	10.99	11.47	30	30	31
22	11.19	11.45	11.68	35	36	37
23	11.19	11.19	11.89	40	39	41
24	11.19	11.19	11.33	45	44	45
25	11.19	11.06	10.88	50	49	48
26	11.19	11.09	11.35	30	31	32
27	11.19	10.89	11.27	35	34	35
28	11.19	11.15	11.24	40	41	41
29	11.19	11.32	11.13	45	46	45
30	11.19	11.58	11.36	50	51	49

The results in Table 3.10 shows that the machine-reported axles spacing range from 10.89 feet to 11.75 feet for EMU3 classifier and 10.10 feet to 12.22 feet for ADR 3000 classifier. In Vehicle B test runs, 17 out of 30 records fall above the ground truth axle spacing of 11.19 feet in EMU3 classifier while the ADR 3000 reported 21 out of 30 records above the ground truth axle spacing.

3.4.2 Graphical Analysis

Figure 3.5 shows the plot for Vehicle A test runs arranged in the order of the run, i.e., from 1 to 29. The results show that there isn't any pattern in the underreporting or overreporting of the axle length for both classifiers. However, both equipment seem to miss the mark consistently. It is difficult to conclude that run #13 is an outlier since the margin of error was the highest for both classifiers. Nonetheless, it would be prudent to remove this run from further analysis to reduce bias in the results.

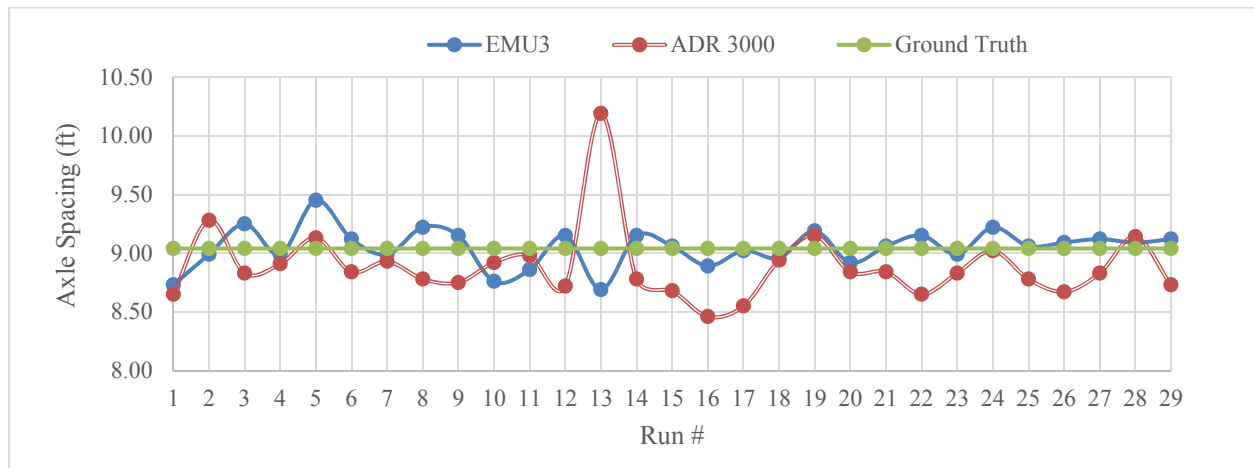


Figure 3.5 Vehicle A Test Runs Plot

Figure 3.6 shows axle spacing plot for test runs for Vehicle B. Again, following visual examination it can be surmised that the readings are all over the place, i.e., not revealing any pattern in overreporting or underreporting. In addition, the differences did not increase with time or decrease with time as test runs were being done. The results, however, show that the ADR 3000 reported an unusually short axle spacing (10.10 feet vs. ground truth of 11.19 feet) in run #4. Thus, we deem this result to be an outlier that should be removed prior to conducting further analysis.

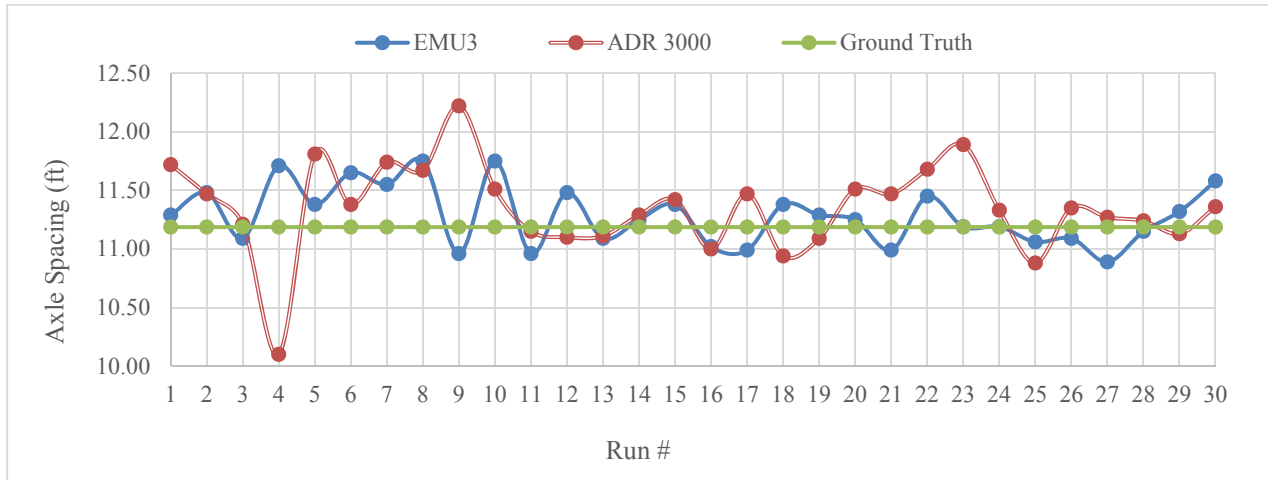


Figure 3.6 Vehicle B Test Runs Plot

3.4.3 Analysis of Reporting Errors

The percentage error for each classifier and for each vehicle runs was calculated as

$$\%Error = \frac{Reported\ Axle\ Spacing - Ground\ Truth\ Spacing}{Ground\ Truth\ Spacing} \times 100$$

The percentage error distributions are plotted in Figure 3.7 to show overreporting and underreporting of the axle spacing. The results show that for Vehicle A test runs the error in reporting range from -3.87% to $+4.54\%$ for EMU3 classifier and from -6.42% to $+12.72\%$ for ADR 3000 classifier. In addition, the results show that for Vehicle B test runs the error in reporting range from -2.66% to $+5.03\%$ for EMU3 classifier and from -9.72% to $+9.23\%$ percent for ADR 3000 classifier. The graph with the combined error plot is displayed in Appendix E.

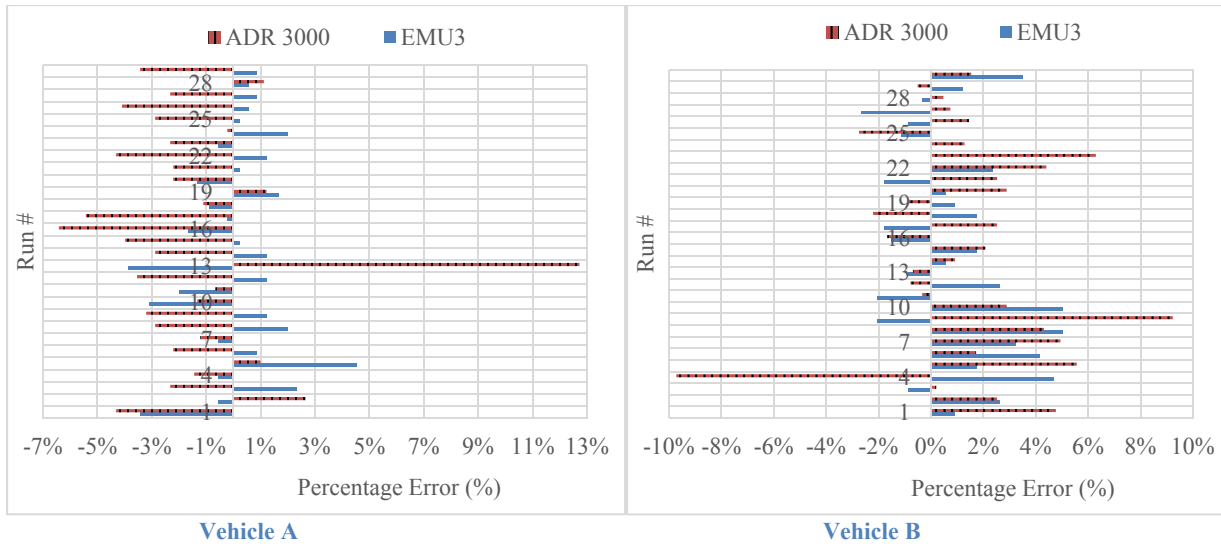


Figure 3.7 Distribution of Errors in Axle Spacing

3.4.4 Statistical Analysis

Table 3.11 summarizes the descriptive statistics on the detected axles spacing for the two equipment types. For Vehicle A, the average axle spacing value from EMU3 is higher than the ground truth value while that of the ADR 3000 being lower. For Vehicle B, both values are higher than ground truth value. The coefficient of variations shows that larger variations are observed in the ADR 3000 classifier (Vehicle A C.V = 2.1% and Vehicle B C.V = 2.7%) than the EMU3 classifier (Vehicle A C.V = 1.7% and Vehicle B C.V = 2.2%). However, it is noteworthy that the coefficients of variation in all cases are well below 10% signify that the equipment are consistent in their sensing of the axle spacing.

TABLE 3.11 Summary Statistics for the Axle Spacing Readings

Statistic	Vehicle A (n = 28)		Vehicle B (n = 29)	
	EMU3	ADR 3000	EMU3	ADR 3000
Maximum	9.45 feet	9.28 feet	11.75 feet	12.22 feet
Average	9.06 feet	8.84 feet	11.27 feet	11.39 feet
Minimum	8.73 feet	8.46 feet	10.89 feet	10.88 feet
Std. Dev.	0.15 feet	0.19 feet	0.24 feet	0.31 feet
Coefficient of Var.	1.7%	2.1%	2.2%	2.7%

Up to this point it is clear that there are differences in how axle spacing lengths are captured. There are differences between reported values and ground truth values. There are also differences between the reported axle spacing lengths by the two classifiers on the same vehicle on the same test run, i.e., inter-equipment differences. To test whether these differences are due to random error or are significant, inferential statistics were conducted as summarized in Table 3.12. The 95% confidence results show that axle spacing reported by ADR 3000 classifier are significantly lower than the ground truth for Vehicle A test runs but they are significantly higher than the ground truth for Vehicle B test runs. EMU3 axle spacing results for both Vehicle A and Vehicle B test runs are within the 95 percent confidence limits. These results are confirmed with the hypothesis

test using t -statistic. The results of the paired t -test as shown in Table 3.12 proves that EMU3 and ADR 3000 have significant differences in reporting axle length of the same vehicle in the same run. The differences were particularly significant for test runs involving Vehicle A (p -value = 0.00).

TABLE 3.12 Inferential Statistics for the Axle Spacing Readings

Statistic	Vehicle A ($n = 28$)		Vehicle B ($n = 29$)	
	EMU3 (ft)	ADR 3000 (ft)	EMU3 (ft)	ADR 3000 (ft)
Error = Ground truth - Avg	-0.02 ft	-0.20 ft	-0.08 feet	+0.20 feet
95% Confidence Interval	9.00 - 9.12 ft	8.77 - 8.92 ft	11.18 - 11.37 ft	11.27 - 11.51 ft
Simple t -test	Ho: $\mu_0 = 9.04$ ft		Ho: $\mu_0 = 11.19$ ft	
	t_{crit}	± 2.05 ft	± 2.05 ft	± 2.05 ft
	t_{stat}	0.79 ft	-5.56 ft	1.57 ft
	p -value	0.44	0.00	0.13
Paired t -test	Ho: $\mu_1 - \mu_2 = 0$ ft			
	t_{crit}	2.05 ft		2.05 ft
	t_{stat}	5.41 ft		-1.83 ft
	p -value	0.00		0.08

3.5 Task 3 Conclusions and Recommendations

Changes in vehicle profiles and upgrades in roadside vehicle classifiers necessitate periodic review of vehicle classification data. The inputs of a classification process together with the classification model used have significant influence on output errors, i.e., vehicles being thrown in the wrong class. The major inputs are the number of axles and axle spacing. This study evaluated how two roadside classifiers, i.e., EMU3 and ADR 3000, reported axle spacing of two vehicles with known axle spacing that were run through the two LPL arrays installed at the Springhill Road test site. The results show that there is within-equipment variation and between-equipment variation on how the axle spacings are captured. For the first test vehicle, Vehicle A, the ADR 3000 classifier reported axle spacings that were significantly lower than the actual ground truth at 95 percent confidence interval. For Vehicle B test runs, the ADR 3000 classifier reported axle spacings that were significantly higher than the actual ground truth at 95 percent confidence interval. Ground truth spacing of both Vehicle A and Vehicle B were within the 95 percent confidence limits of EMU3 axle spacing results. The paired t -test showed that axle spacing reading are significantly different between the two classifiers on the same vehicle. These results suggest that improper capturing of axle spacings contribute to errors in vehicle classification data particularly on classes with tight axle spacing thresholds.

As indicated earlier, the classification model also has influence on output errors. The Florida DOT classification scheme uses axle spacing thresholds for various classes and a decision tree in which the order of the algorithm in placing vehicles in a particular class is followed. Minor

but consequential differences were observed among vendors on how they implement the thresholds and decision tree. Although most axle spacing limits implemented by vendors were similar to the current FDOT classification table limits, minor differences were noticed in Class 2, 8, 9, and 13. In addition, there were differences in the class trees. Previous studies have shown that optimization of class trees can improve classification accuracy by up to 3 percent.

Based on the above results and the review of the Florida DOT Traffic Monitoring Handbook (TMH), it is recommended that uniformity of operation among vendors is essential and can be achieved through revision of the TMH following a detailed study of vehicle classification from a number of production sites across the state. It can be surmised that the current FDOT TMH does not specifically require vendors to strictly adhere to axle spacing thresholds in all classes or to strictly use a particular decision tree. The required annual certification accuracy just states that the volume counts and axle classification in four main groups should be within 10 percent of the ground truth. These requirements may be too broad given the advancement of vehicle sensing and microcomputing technologies. It is therefore suggested that further study on this issue is warranted.

3.6 References

- Florida Department of Transportation. (2018). *FDOT Traffic Monitoring Handbook*. Florida Department of Transportation, Tallahassee, FL.
- Masaki, J. E. (2016). *Evaluation of Florida Vehicle Classification Table* (Master's Thesis). Florida State University, Tallahassee, FL.
- Refai, H., Bitar, N., Schettler, J., & Kalaa, O. A. (2014). *The Study of Vehicle Classification Equipment with Solutions to Improve Accuracy in Oklahoma*. Oklahoma Department of Transportation, Oklahoma City, OK.

TASK 4: EVALUATION OF PED-BIKE MONITORING SYSTEMS

4.1 Purpose and Scope

Sound processes and procedures in traffic data collection are important as most infrastructure owners and operators (IOO) embark on counting both motorized (vehicular) traffic and non-motorized (ped-bike) traffic. It is important that roadside data recorders are capable of interpreting and recording vehicular and non-vehicular traffic in an integrated manner. Initially, the aim of this task was to evaluate product features; to evaluate integration capabilities of a recorder with other systems; to determine data characteristics produced by the recorder; and to determine field test and calibrations procedures. However, because of operational delays in detection systems calibration and verification, the task reported herein was mainly aimed at operational evaluation of the bike-ped detection systems installed at Site 9900. As more products for motorized and non-motorized traffic come into the market, future research efforts will be directed at evaluating their efficacy for Florida use.

4.2 Study Site

The testbed located at the Capital Circle Highway was utilized in this study. The testbed is designated as TTMS Site 9900 and was established in September 2014 for the purpose of consolidating field evaluations – that were scattered throughout the state at that time – to one location; conducting short-term and long-term evaluation of piezos, loops, and sealants as well as conducting long term evaluation of WIM sensors. The testbed has also been equipped with the capability to evaluate intrusive and non-intrusive sensors and the accompanying data loggers. Figure 4.1 shows the setup of the test site.

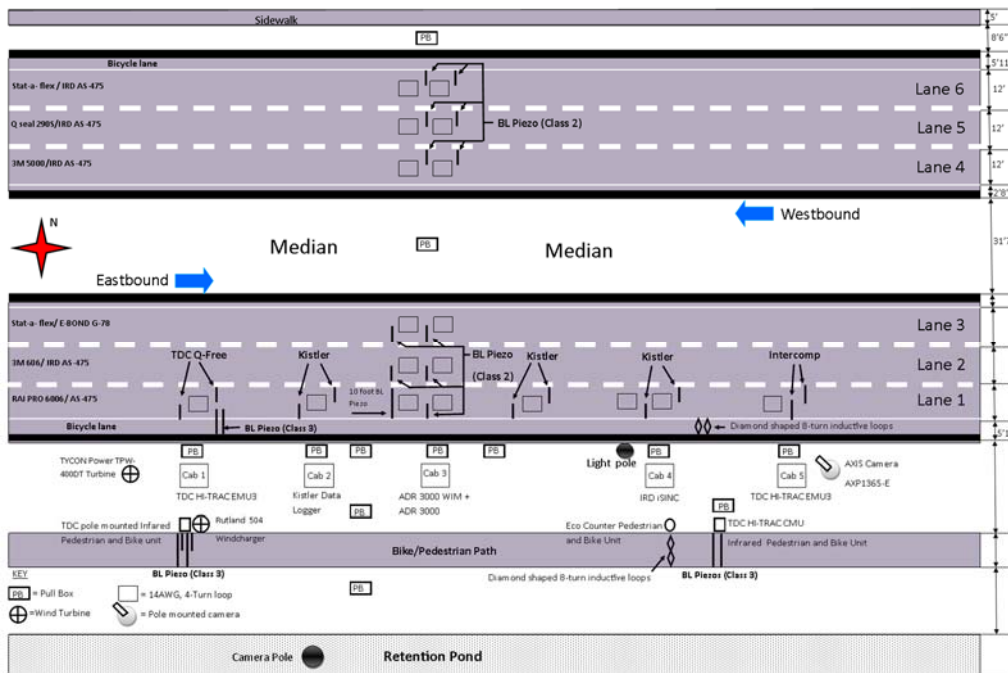


Figure 4.1 Setup of Data Collection Equipment at Site 9900

As can be seen in Figure 4.1, there are a number of sensor configurations that can be used to study the efficacy of these sensors in collecting motorized and non-motorized traffic. The following sections discuss in sufficient detail the technology of used by the four ped-bike detection systems installed at Site 9900.

4.3 Ped-Bike Systems

The review of the current state-of-the-art and the state-of-practice revealed that there are many systems in the market geared towards collection and monitoring of pedestrian and bicycle activities on shared lanes, dedicated lanes, and on trails such as the one existing on the Capital Circle Road. Different vendors use different detection technologies. Some vendors have both mobile (temporary) detection systems and permanent detection systems while other vendors have one type only. The following subsections describes the systems that were installed at the test site for evaluation purposes. The description relies mostly on the manufacturer’s data sheet and is mainly on the technology used and bike-ped attributes that are collected by each system.

4.3.1 RidePod BT Bike Tube Counter by MetroCount

The RidePod BT Bike Counter by *MetroCount* uses thin-walled pneumatic tubes to detect bike axles. Two pneumatic tubes are generally fixed 1.5 feet apart, perpendicular to the bike lane. Since the bike has two wheels and the counter connects to two tubes, the system records four hits per bike. As the tube counters are secured above the pavement using tapes and nails, it is therefore a temporary counting device. It is worth noting that the company, *MetroCount*, informed the research team that they now have a permanent bike counting system but it was not part of this research study.

The manufacturer’s datasheet indicated that the counter is able to collect volume, speed, direction, and bike headways. In addition, the datasheet indicated that the counter can detect clusters of bicyclist traveling in proximity to each other. Figure 4.2 shows the set-up of the RidePod BT Bike Tube counter at Site 9900 while Appendix F shows the product data sheet.



Figure 4.2 RidePod BT Bike Tube Counter

4.3.2 HI-TRAC OH-PED by Q-Free

The HI-TRAC OH-PED is an overhead pedestrian detection system that, according to the manufacturer, **when combined with the HI-TRAC CMU** bike detection system provides a highly accurate and robust detection of non-motorized traffic. Similar to the CMU setup, the system uses piezoelectric or loop sensor technology to detect bicycle activity. As for pedestrian detection, the system has an overhead optical device that detects the heat emitted by people passing underneath as infrared radiation through germanium lens. It is generally installed to have a square sensing area on the pavement, the area being directly proportional to the mounting height. The system is claimed to be able to collect bicyclist volumes, pedestrian volumes, speed, and headways. Figure 4.3 shows the HI-TRAC OH-PED field set-up while Appendix G shows the product data sheet.



Figure 4.3 Field Setup of HI-TRAC OH-PED Counter

4.3.3 Urban Post MULTI by Eco-Counter

According to the manufacturer, i.e., *Eco-Counter*, the Urban Post MULTI is a permanent pedestrian and bike counter for use in urban environment including shared paths with pedestrians in the sidewalk and cyclist using an adjacent bike lane. The Urban Post MULTI system combines two technological applications to differentiate between pedestrians and bicyclists. Pedestrians are detected by a passive infrared beam which detects a change in the thermal contrast caused by a pedestrian passing within a defined field of vision. Bicycling activity is detected using inductive loop sensors buried in the pavement in a particular configuration.

Besides the ability to differentiate between pedestrians and cyclists, the manufacturer's datasheet indicates that the system can detect the direction of travel. Figure 4.4 shows the setup of Urban Post MULTI counter at Site 9900 while Appendix H shows the product data sheet.

4.3.4 HI-TRAC CMU by Q-Free

The HI-TRAC CMU system is claimed by the manufacturer that it is capable of monitoring a combination of bicycle lanes and pedestrian sidewalks and trails. It is further claimed that bicycles can be detected in separate (dedicated) bicycle lanes or in lanes shared by vehicles and bicycles. The system uses piezoelectric or loop sensor technology to detect bicycle activity and pyroelectric infrared sensors to detect pedestrian activity. However, the manufacturer's datasheet indicates that the pedestrian detection using pyroelectric infrared sensors is optional. According to the datasheet, bicycles made of non-metallic materials including carbon fiber can be detected by this system.

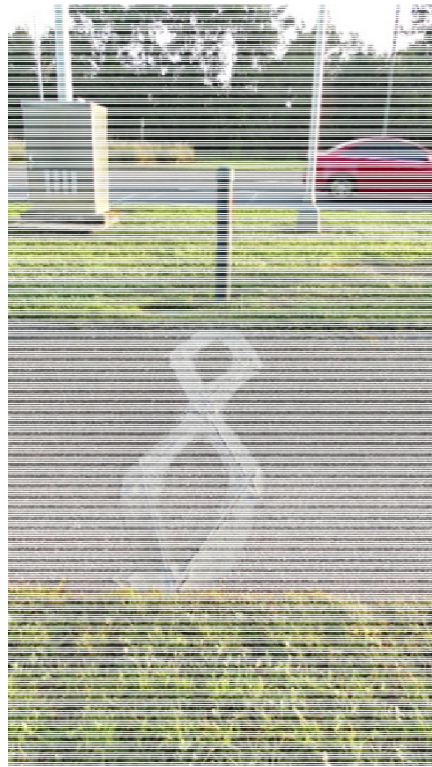


Figure 4.4 Urban Post MULTI counter

With piezo sensor configuration, the piezoelectric sensors are installed between 1 to 3 feet apart in the cycle or vehicle lane surface. The piezoelectric sensor outputs electrical charge proportional to the applied pressure of a vehicle axle or wheel passing over it. Thus, this set-up can collect pedestrian and bicycle passage attributes including date, time, lane, class, gap, and speed. Figure 4.5 shows the HI-TRAC CMU set-up while Appendix I shows the product data sheet.



Figure 4.5 HI-TRAC CMU Setup

4.4 Research Design

As indicated earlier, the purpose of this study was to evaluate the effectiveness of various ped-bike detection systems in collecting the non-vehicular data. Since the four systems are installed side-by-side at Site 9900, this afforded the research team the opportunity to conduct comparative analysis of the four systems. Volunteers were recruited to ride bicycles over the four systems and to walk as pedestrians over the four systems. The bicyclists and pedestrians were asked to hit the sensors at various lateral locations; to cross the sensors individually and in groups; and to cross the sensors at different speeds ranging from low to high.

Video data was being collected as the bicyclists and the pedestrians were passing over the four detection systems. The research was designed such that the data captured and recorded by the individual systems were to be compared with the data extracted from the videos. The data extracted from the videos were to be considered as the ground truth. The variables of interest in this study included bike and ped volumes per time period, speed, and clustering detection.

4.5 Data Extraction and Analysis

Prior to collecting data in the field, the units had to be calibrated per manufacturer's recommendation. This was done on a couple of days prior to field data collection. The research study was conducted on July 18, 2019 beginning at 8 a.m. Eight people volunteered to participate in the study. The study proceeded as follows. All volunteers rode bikes over the four detection systems from 8:00 a.m. to 8:30 a.m. Between 8:30 a.m. and 8:45 a.m. the riders were requested to try as much as possible to arrive at a sensor location at the same time in order to evaluate the ability of a sensor to simultaneously detect multiple subjects traveling in the same direction or in opposite direction. After a 5-minute break, the study resumed from 8:50 a.m. to 9:20 a.m. in which

some volunteers switched to pedestrian mode and a few continued in bicyclist mode. In-between this time period some pedestrians and some bicyclists were asked to arrive and hit the sensor simultaneously for the purpose of determining the ability of the sensor to differentiate between a pedestrian and a bicyclist arriving in the detection zone at the same time. Figure 4.6 shows the simultaneous arrival of pedestrians and/or bicyclists. Again, as indicated earlier, volunteers were asked to sometimes cross the sensors individually and sometimes in groups and at different speeds.

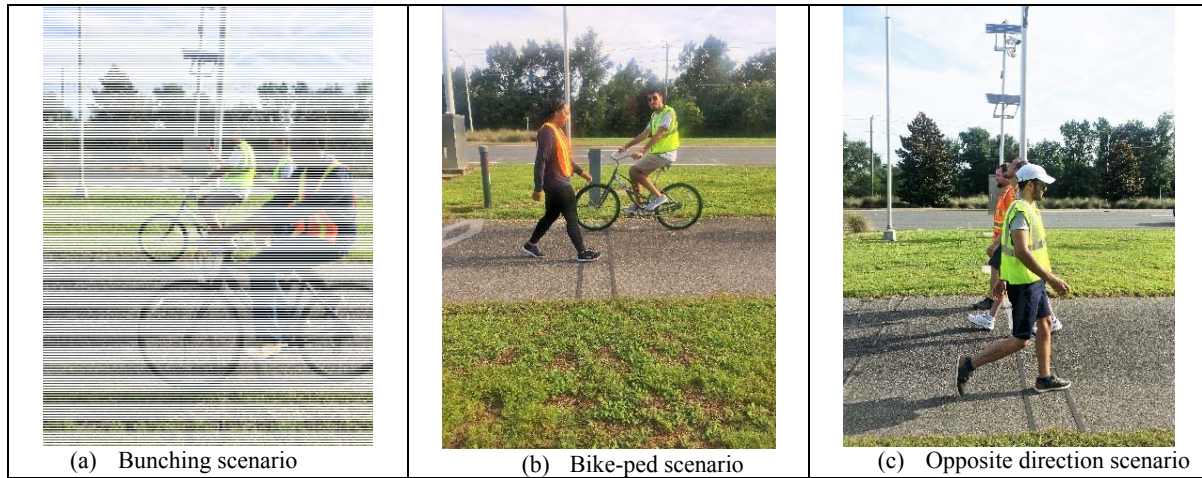


Figure 4.6 Various test scenarios

The Florida DOT personnel involved in the study downloaded the data from all four detection systems and provided them to the research team. In the meantime, the research team embarked on a meticulous task of extracting various data attributes from the videos that were collected during the study period.

4.5.1 MetroCount Analysis

Appendix J shows the snapshot of raw data extracted from the recorded videos that are being using as the ground truth in the comparative analysis. The time-stamped video events were matched with the time-stamped Metrocount events. Table 4.1 shows the results of the events matching.

TABLE 4.1 Results of MetroCount Bicyclists Detection

	<i>N</i>	<i>Accuracy with clustering</i>	<i>Accuracy without clustering</i>
Counts from video			
Correct counts by Metrocount	354	87.6%	94.7%
Counts missed by Metrocount due to clustering	30		
Total missed counts	50		

The results in Table 4.1 shows that there were a total of 404 bicyclists crossing the MetroCount pneumatic tubes in the east and west direction of which 354 (87.6%) were correctly detected.

However, of the 50 missed detections by Metrocount, 30 counts were missed because of clustering. If clustering (defined as bicyclist arriving on the pneumatic tube with a headway of ≤ 1 second) is not considered, the accuracy improves to 94.7% $[354 \times 100 \div (404 - 30)]$. The results further showed that the total MetroCount events were 446 which is 42 more than the actual number of bicyclists that crossed the tubes as seen in the videos. Closer examination of the videos indicated that during the pedestrian walking phase of the project, some pedestrians were stepping on the tubes thus triggering false detection. Most of these false triggers resulted in low recorded speeds, approximately less than 1 mph. A number of issues were observed during field data collection and data analysis including the fact that there was one tricyclist that was counted as a bicyclist by MetroCount.

4.5.2 HI-TRAC OH-PED Analysis

Unlike Metrocount system analyzed in Section 4.5.1 above, the HI-TRAC OH-PED system is designed to detect both bicyclists and pedestrians. Metrocount system that was evaluated at Site 9900 detects bicyclists only. As discussed earlier, the HI-TRAC OH-PED utilizes surface mounted piezoelectric sensors to detect bicycles as they press on the piezoelectric material. Pedestrians are detected within the designated detection zone when infrared heat generated by the human body is picked up by the overhead infrared sensor. Figure 4.7 shows the results of the comparative analysis between video and HI-TRAC OH-PED detection of bicyclists and pedestrians. Again, the snapshot of raw data from which the counts were extracted are shown in Appendix D.

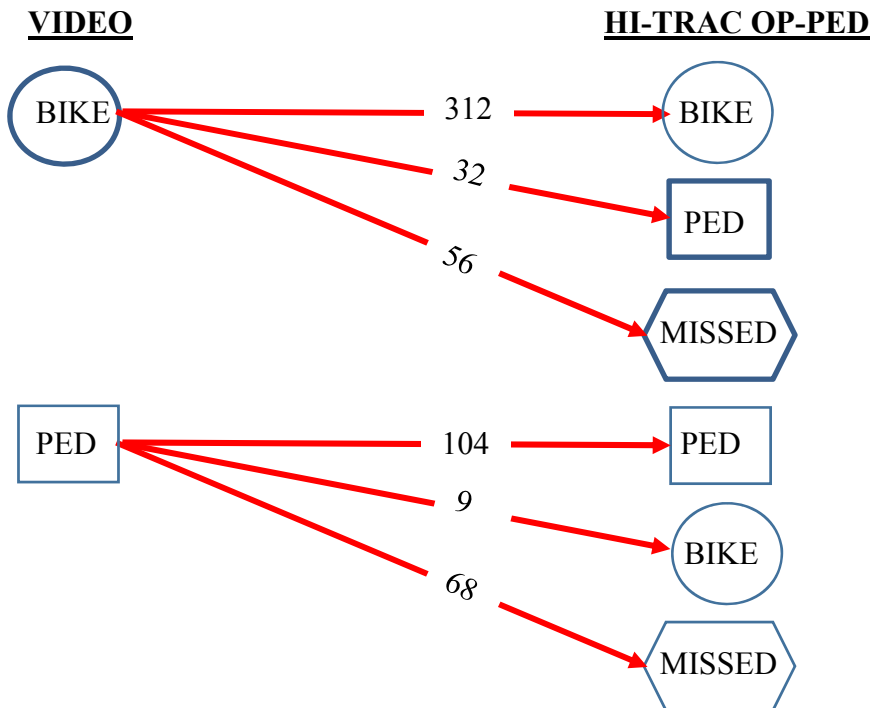


Figure 4.7 Performance Analysis of HI-TRAC OP-ED bike-ped system

Based on video data, the results in Figure 4.7 shows that 400 bicyclists crossed the HI-TRAC OH-PED underground piezoelectric sensor during the study time period. Of the 400 actual bicyclists that crossed the sensor, 312 bicyclists were correctly detected as bicyclists, 32 were incorrectly

sensed as pedestrians, and a total of 56 bicyclists were not detected at all, i.e., missed detections. Based on these numbers, it can be surmised that the accuracy of the HI-TRAC OH-PED in detecting bicyclists is 78%. However, there is a caveat to this detection accuracy. Even though 312 bicycling events were correctly detected, 31 of these events were direction-wise incorrectly detected – that is, 26 bicyclists traveling westbound were incorrectly reported as travelling eastbound, while 5 eastbound bicyclists were incorrectly labeled as traveling westbound.

Closer look at the 32 incorrectly detected bicyclists and 56 missed detections revealed the following. All 32 bicycling events classified as pedestrians occurred when the speed was recorded as being under 3 mph. It was later learned that the system was set up to classify low-speed events, i.e., less than 3 mph, as pedestrians. As for the 56 missed bicyclist detections, the review of the video showed that when bicyclists were crossing the piezoelectric sensors in clusters (i.e., two to three bicyclists crossing at the same time), only one event (i.e., one bicyclist) was captured by the sensor. There were 40 missed detections due to clustering. Thus, if those clustering bicycling events weren't there on the video, the accuracy of HI-TRAC OH-PED bike detection improves to 86.7% [$312 \times 100 \div (400 - 40)$].

The results in Figure 4.7 further show that 181 pedestrians crossed the infrared detection zone during the analysis period. Of these 181 pedestrians, 9 were incorrectly recorded as bicyclists, and 56 were missed by the sensor altogether. These figures represent a detection rate of 57.5%. Again, there is an important caveat to this detection rate figure. Of the 104 correctly detected pedestrians, 25 were directionally incorrect: 15 were detected as eastbound while actually traveling westbound and 10 were incorrectly reported as traveling westbound. The high number of missed detections might have occurred because of the “clustering effect” in which a number of pedestrians were crossing the detection zone in pairs and sometimes in a group of three and four people. There were 32 such pedestrian events counted on the video that were missed by the HI-TRAC OH-PED. Thus, the accuracy of the system without clustering can be said to be 69.8% [$104 \times 100 \div (181 - 32)$]. The research team was advised that there is a “clustering” feature in the HI-TRAC OH-PED software that was not activated. If turned on, it was said that this feature could help correctly identify individuals in a cluster.

4.5.3 *EcoCounter Urban Post MULTI Analysis*

The *Urban Post MULTI* detection system by EcoCounter detects bicycling events using inductive loop sensors buried in the pavement and detects pedestrian events using a horizontal passive infrared beam. Data are collected by the system and stored in a roadside counter. However, the EcoCounter counter does not provide time-stamped individual bike events and instead aggregates the data in 15-minute periods as shown in Table 4.2.

Table 4.2 shows that the video count of bicyclists was 371 in the analyzed one-hour period. During this time, the EcoCounter reported a total of 335 bicyclists, representing a weighted detection rate of 90.3%. On the other hand, the video count of pedestrians in the one-hour period was 72 while the EcoCounter reported 70. However, 22 of the pedestrians reported by EcoCounter in the 8 a.m. to 8:45 a.m. time period are “ghosts” as the review of the video showed that no pedestrian crossed the EcoCounter loops during this time period. Thus, the weighted accuracy level is 66.7%. It is difficult to ascertain the actual accuracy level of the EcoCounter Urban Post

MULTI system because of data aggregation. Proper accuracy determination required individual records to enable one-to-one matching of bicyclists and pedestrians.

TABLE 4.2 Results of EcoCounter Pedestrians and Bicyclists Detection

Time	Detector	Bicyclists				Pedestrians			
		EB	WB	Total	Accuracy	EB	WB	Total	Accuracy
8:00 – 8:15	Video	60	64	124	88.7%	0	0	0	0.0%
	EcoCounter	52	58	110		3	8	11	
8:15 – 8:30	Video	68	70	138	92.0%	0	0	0	0.0%
	EcoCounter	64	63	127		2	5	7	
8:30 – 8:45	Video	37	40	77	88.3%	0	0	0	0.0%
	EcoCounter	31	37	68		1	3	4	
8:45 – 9:00	Video	16	16	32	93.8%	35	37	72	66.7%
	EcoCounter	17	13	30		29	19	48	
Weighted					90.3%	Weighted			66.7%

4.5.4 HI-TRAC CMU Analysis

The HI-TRAC CMU and HI-TRAC OH-PED are both products of Q-Free Company and utilize the same piezoelectric sensor principle to detect bicycle hits. The difference is in the pedestrian detection in which HI-TRAC CMU utilizes a horizontal infrared beam that triggers detection when the beam is crossed. Figure 4.8 shows the results of the performance evaluation of the HI-TRAC CMU bike-ped detection system. The results in Figure 4.8 show that a total of 391 bicyclists crossed the underground piezo sensors at this location based on the data extracted from the video. Out of 391 bicyclists, 289 were correctly classified while 48 were incorrectly classified as pedestrians and a total of 54 bicyclists were missed by the HI-TRAC CMU system. This represents a bike detection rate of 74%.

One qualification though of this accuracy is that of the 289 correctly detected bicyclist events, 28 were directionally incorrect (i.e., 20 were incorrectly reported as eastbound while 8 were incorrectly reported as westbound). Closer examination of the 48 misidentified bicycling events and the 54 missed detections revealed a pattern similar to HI-TRAC OH-PED in which low speed bicyclists were classified as pedestrians and clusters of bicycles were missed. In fact, a total of 33 bicycling clustering events that were seen on video were missed by the HI-TRAC CMU. If these clustering events weren't there, the accuracy of the HI-TRAC CMU bicyclist detection improves to 80.7% [$289 \times 100 \div (391 - 33)$].

As for pedestrian detection, Figure 4.8 shows that, based on the data extracted from the videos, 148 pedestrians crossed the HI-TRAC CMU piezos during the analysis period. Of the 148 pedestrian events, 101 were correctly detected, 5 were classified as bicyclists, and 42 pedestrians were not detected by the system. This represents a pedestrian detection rate of 68.2%. Again, the caveat in this case is that 9 of the 101 correct pedestrian detections were directionally incorrect –

3 were incorrectly reported as eastbound and 6 were incorrectly reported as westbound. Closer review of the 5 misclassified pedestrians and 42 undetected pedestrians revealed that when pedestrians and bicyclists were clustered within the detection zone, some pedestrians were classified as bicyclists and some went undetected. Pedestrians that went undetected due to clustering were 25 as counted on video representing an accuracy of 82.1% [$101 \times 100 \div (148 - 25)$] for the HI-TRAC CMU system if clustered events are removed from the counts.

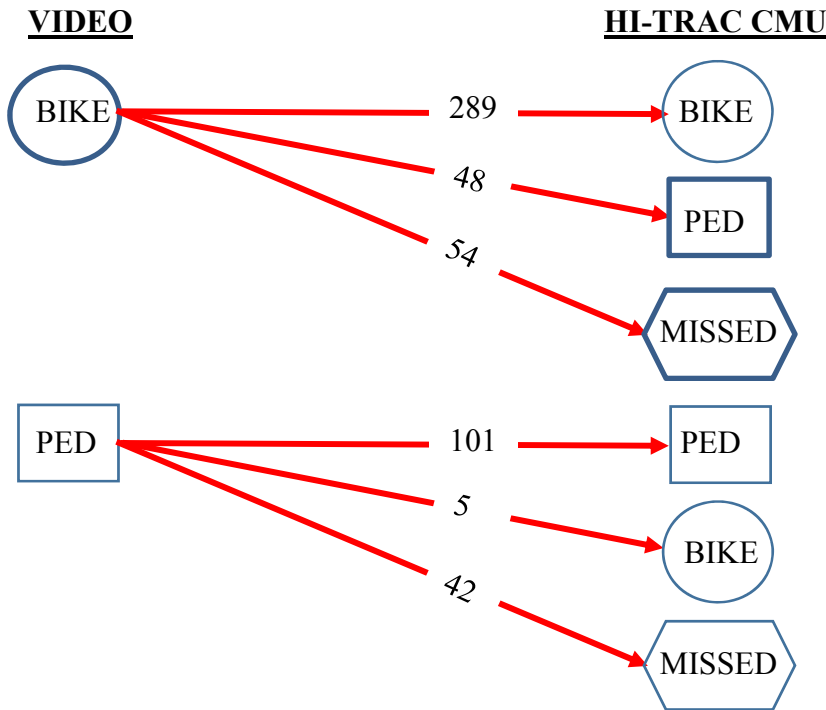


Figure 4.8 Performance Analysis of HI-TRAC CMU bike-ped sensing system

4.6 Task 4 Conclusions & Recommendations

Consistent with FDOT Transportation Data and Analytics Office goal of continually improving equipment, processes and procedures for traffic data collection, the main goal of this task was to conduct operational evaluation of the four bike-ped detection systems installed at Site 9900. These systems were RidePod BT Bike Tube Counter by *MetroCount*, HI-TRAC OH-PED by *Q-Free*, Urban Post MULTI by *EcoCounter*, and HI-TRAC CMU also by *Q-Free*. Several bike-ped runs were undertaken across all systems. A video camera was used to record and later extract time-stamps of individual bike-ped events at each system. The video data was used as ground truth to compare with data downloaded from each system's storage device.

The results showed that different levels of accuracy were achieved by the four systems in detecting bicycling events and pedestrian events. The bicyclist detection accuracy ranged from the low of 74% reported by *Q-Free's* HI-TRAC CMU detection system to the high of 90.3% reported by *EcoCounter's* Urban Post MULTI detection system. The pedestrian detection accuracy level ranged from the low of 57.5% associated with *Q-Free's* HI-TRAC OH-PED detection system to the high of 68.2% associated with *Q-Free's* HI-TRAC CMU detection system. It is noteworthy that the *MetroCount* pneumatic tube counters are not designed to detect

pedestrians. It is also worth noting that the accuracy of the *EcoCounter* detection system was not evaluated on similar basis because the counter reports the bike-ped data in 15-minute intervals rather than individual time-stamped records. Thus, it is difficult to ascertain the degree to which some bicyclists were reported as pedestrians and vice versa.

There are a few limitations of this study that need to be highlighted as well as recommendations for improvement. This study did not evaluate camera-based bike-ped detection systems because of contractual and time limitations. The cursory review of literature revealed that there are camera-based detection systems that have produced reasonable detection rates. It is recommended that as these products come to the market, future research studies should include camera-based bike-ped detection systems. In addition, some of the bikes used in this study were of carbon-fiber material and it is not clear the influence of this factor on detection accuracy as it was not evaluated. Moreover, practically all systems that detect pedestrians had difficulty in detecting pedestrians crossing in cluster of 2, 3 or more people. It has been suggested that some of the detection systems do have a feature that could improve identifying the number of individuals in a cluster. It is recommended that the efficacy of such feature be evaluated in future studies. Finally, it is recommended that the ability of these and other detection systems to collect data in bike-ped-vehicle shared lane environment be evaluated as it was not covered in this study.

APPENDIX A – CAT Scale Certification

56796637
TICKET NUMBER

CAT SCALE
CERTIFIED AUTOMATED TRUCK SCALE

CAT SCALE COMPANY
P.O. BOX 630
WALCOTT, IA 52773
(563) 284-6263
www.catscale.com

THE CAT SCALE GUARANTEE
The CAT Scale Company guarantees that our scales will give an accurate weight. What makes us different from other scale companies is that we back up our guarantee with cash.

WEIGH WHAT WE SAY OR WE PAY
If you get an overweight fine from the state **AFTER** one of our CAT Scales showed a legal weight, we will immediately check our scale and we will:
(1) Reimburse you for the cost of the overweight fine if our scale is wrong, **OR**
(2) A representative of CAT Scale Company will appear in court **WITH** the driver as an expert witness if we believe our scale was correct.

IF YOU SHOULD GET AN OVERWEIGHT FINE, YOU SHOULD DO THE FOLLOWING TO GET THE PROBLEM RESOLVED:
1) Post bond and request a court date.
2) Call CAT Scale Company direct 24 hours a day at 1-877-CAT-SCALE, ext. 7 (Toll Free) or visit www.catscaleguarantee.com for instructions.
3) **IMMEDIATELY** send a copy of the citation, CAT Scale Ticket, your name, company, address, and phone number to CAT Scale Company Attn: Guarantee Department.

*The four weights shown below are separate weights. The GROSS WEIGHT is the CERTIFIED WEIGHT and was weighed on a full length platform scale. All weights are guaranteed by CAT Scale.

DATE: 2-04-19

STEER AXLE 11040 lb
DRIVE AXLE 31900 lb
TRAILER AXLE 34300 lb
* GROSS WEIGHT 77240 lb

14:27 SCALE: 1422
56796637 LOCATION: FLYING J PILOT
PUBLIC WEIGH-MASTERS CERTIFICATE OF WEIGHT & MEASURE I 10 EXIT 192
MIDWAY FL

IMPRINT SEAL HERE (IF APPLICABLE)

LIVESTOCK, PRODUCE, PROPERTY, COMMODITY, OR ARTICLE WEIGHED **FREIGHT ALL KINDS**

COMPANY **FDOT** TRACTOR # **30360** TRAILER # **0652**

WEIGH NUMBER **6637** FEE \$11.50 WEIGHMASTER OR WEIGHER SIGNATURE *Tiffany Donaldso* TICKET # OF FULL S WEIGH (IF REWEIGH) **TIPPANY DONALDSON**

CUSTOMER COPY © CAT Scale® Reg 3067 7/18

56796688
TICKET NUMBER

CAT SCALE
CERTIFIED AUTOMATED TRUCK SCALE

CAT SCALE COMPANY
P.O. BOX 630
WALCOTT, IA 52773
(563) 284-6263
www.catscale.com

THE CAT SCALE GUARANTEE
The CAT Scale Company guarantees that our scales will give an accurate weight. What makes us different from other scale companies is that we back up our guarantee with cash.

WEIGH WHAT WE SAY OR WE PAY
If you get an overweight fine from the state **AFTER** one of our CAT Scales showed a legal weight, we will immediately check our scale and we will:
(1) Reimburse you for the cost of the overweight fine if our scale is wrong, **OR**
(2) A representative of CAT Scale Company will appear in court **WITH** the driver as an expert witness if we believe our scale was correct.

IF YOU SHOULD GET AN OVERWEIGHT FINE, YOU SHOULD DO THE FOLLOWING TO GET THE PROBLEM RESOLVED:
1) Post bond and request a court date.
2) Call CAT Scale Company direct 24 hours a day at 1-877-CAT-SCALE, ext. 7 (Toll Free) or visit www.catscaleguarantee.com for instructions.
3) **IMMEDIATELY** send a copy of the citation, CAT Scale Ticket, your name, company, address, and phone number to CAT Scale Company Attn: Guarantee Department.

*The four weights shown below are separate weights. The GROSS WEIGHT is the CERTIFIED WEIGHT and was weighed on a full length platform scale.

DATE: 2-06-19

STEER AXLE 11100 lb
DRIVE AXLE 31920 lb
TRAILER AXLE 34660 lb
* GROSS WEIGHT 77700 lb

SCALE: 1422
LOCATION: FLYING J PILOT
PUBLIC WEIGH-MASTERS CERTIFICATE OF WEIGHT & MEASURE I 10 EXIT 192
MIDWAY FL

IMPRINT SEAL HERE (IF APPLICABLE)

LIVESTOCK, PRODUCE, PROPERTY, COMMODITY, OR ARTICLE WEIGHED **FREIGHT ALL KINDS**

COMPANY **FDOT** TRACTOR # **30361** TRAILER # **0640**

WEIGH NUMBER **6688** FEE \$11.50 WEIGHMASTER OR WEIGHER SIGNATURE *Clayton* TICKET # OF FULL S WEIGH (IF REWEIGH) **CLAYTON**

CUSTOMER COPY © CAT Scale® Reg 3067 7/18

APPENDIX B – Test Runs

Run	DATE	TIME	SPEED	WEIGHTS (pounds)				AXLE SPACINGS (feet)			
				GVW	STEER AXLE	DRIVE AXLE	TRAILER AXLE	AXLE 1-2	AXLE 2-3	AXLE 3-4	AXLE 4-5
1	2/5/2019	14:57:34	38.1	77140	10670	32,738	33,732	15.6	4.45	20.55	4.4
2	2/5/2019	15:06:51	39.4	77624	10934	33,312	33,378	15.7	4.5	20.75	4.4
3	2/5/2019	15:14:05	39.4	76876	10758	32,914	33,202	15.5	4.45	20.55	4.35
4	2/5/2019	15:21:38	38.8	76698	10472	32,496	33,732	15.5	4.5	20.55	4.35
5	2/5/2019	15:29:17	38.8	76654	10384	32,628	33,642	15.55	4.45	20.5	4.4
6	2/5/2019	15:37:31	43.8	76302	11090	32,144	33,070	15.55	4.45	20.65	4.4
7	2/5/2019	15:45:16	44.4	76654	10934	32,430	33,288	15.55	4.45	20.55	4.35
8	2/5/2019	15:57:00	44.4	75684	11354	31,946	32,386	15.5	4.5	20.55	4.45
9	2/5/2019	16:04:46	45	78088	10934	32,144	35,010	15.55	4.5	20.55	4.4
10	2/5/2019	16:13:48	44.4	77294	11112	32,738	33,444	15.6	4.45	20.65	4.4
11	2/6/2019	9:21:06	49.4	79498	11706	34,194	33,600	15.6	4.55	20.75	4.35
12	2/6/2019	9:28:26	50	80800	11222	33,996	35,582	15.65	4.55	20.75	4.4
13	2/6/2019	9:35:07	49.4	79896	11750	33,576	34,568	15.6	4.5	20.7	4.4
14	2/6/2019	9:42:12	49.4	81792	11508	34,194	36,090	15.6	4.5	20.75	4.4
15	2/6/2019	10:00:45	49.4	80138	11420	33,688	35,032	15.55	4.5	20.7	4.35
16	2/6/2019	10:09:25	40	78860	11662	33,862	33,334	15.7	4.5	20.85	4.45
17	2/6/2019	10:17:41	35	79454	10956	33,290	35,208	15.7	4.55	20.75	4.4
18	2/6/2019	10:25:19	43.8	80556	11816	33,422	35,318	15.6	4.55	20.8	4.45
19	2/6/2019	10:31:47	40.6	79454	11662	34,988	32,806	15.7	4.5	20.85	4.4
20	2/6/2019	10:44:26	35.6	78066	11332	32,760	33,974	15.7	4.5	20.8	4.4
21	2/6/2019	10:52:07	48.8	80468	11376	33,710	35,384	15.6	4.5	20.75	4.4
22	2/6/2019	10:59:33	44.4	79036	11442	33,334	34,260	15.6	4.5	20.75	4.4
23	2/6/2019	11:07:26	35	78110	11244	32,936	33,930	15.7	4.55	20.8	4.45
24	2/6/2019	11:15:47	44.4	78088	11376	33,026	33,686	15.65	4.55	20.8	4.45
25	2/6/2019	11:23:53	40	78264	10780	33,820	33,664	15.6	4.55	20.65	4.35
26	2/6/2019	11:31:33	54.4	80028	11244	33,422	35,362	15.7	4.55	20.9	4.4
27	2/6/2019	11:40:56	50	80138	11090	33,510	35,538	15.6	4.45	20.75	4.4
28	2/6/2019	11:48:26	54.4	78484	11552	32,342	34,590	15.6	4.5	20.75	4.4
29	2/6/2019	12:04:12	53.1	79212	11046	32,738	34,194	15.6	4.55	20.75	4.45
30	2/6/2019	12:11:18	53.8	78440	12302	33,730	34,436	15.7	4.55	20.9	4.45

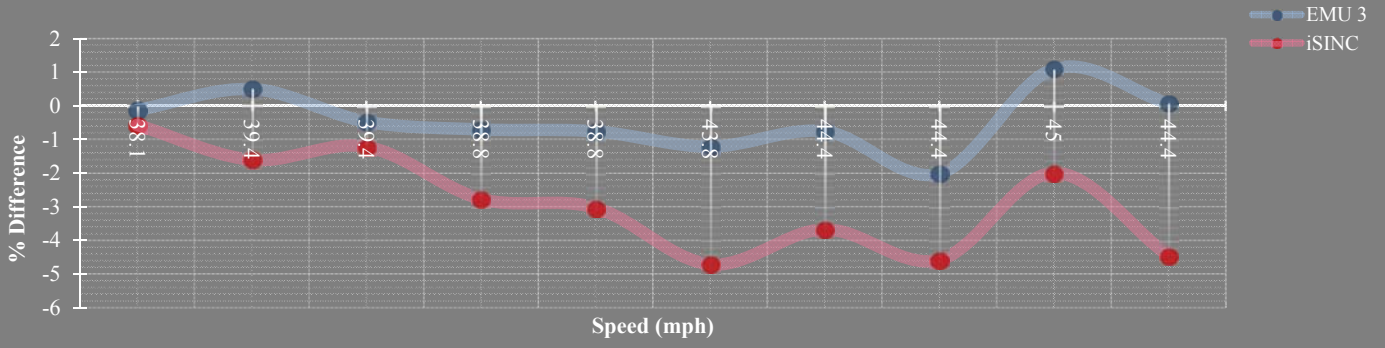
				ISINC ON EAST ARRAY									
Run	DATE	TIME	SPEED	WEIGHTS (pounds)				AXLE SPACINGS (feet)					
				GVW	STEER AXLE	DRIVE AXLE	TRAILER AXLE	AXLE 1-2	AXLE 2-3	AXLE 3-4	AXLE 4-5		
1	2/5/2019	14:57:34	38.1	76,800	11,700	32,500	33,500	15.9	4.7	21.1	4.5		
2	2/5/2019	15:06:51	39.4	76,000	10,700	32,800	32,500	15.9	4.7	21.2	4.5		
3	2/5/2019	15:14:05	39.4	76,300	11,000	32,500	32,900	15.8	4.6	21	4.6		
4	2/5/2019	15:21:38	38.8	75,100	10,700	32,100	32,400	15.8	4.7	21.1	4.5		
5	2/5/2019	15:29:17	38.8	74,900	10,300	32,200	32,400	15.9	4.6	21.2	4.5		
6	2/5/2019	15:37:31	43.8	73,600	10,500	31,900	31,200	15.9	4.6	21.2	4.6		
7	2/5/2019	15:45:16	44.4	74,400	10,700	31,100	32,500	15.8	4.6	21.1	4.5		
8	2/5/2019	15:57:00	44.4	73,700	10,600	31,600	31,700	15.8	4.6	21.1	4.5		
9	2/5/2019	16:04:46	45	75,700	10,700	32,500	32,500	15.8	4.6	21.2	4.5		
10	2/5/2019	16:13:48	44.4	73,800	10,900	31,200	31,800	15.9	4.6	21.1	4.6		
11	2/6/2019	9:21:06	49.4	76,400	11,400	32,800	32,200	15.7	4.5	20.8	4.5		
12	2/6/2019	9:28:26	50	79,600	11,600	33,500	34,500	15.8	4.6	21	4.5		
13	2/6/2019	9:35:07	49.4	77,400	11,600	32,800	32,900	15.7	4.6	20.9	4.5		
14	2/6/2019	9:42:12	49.4	78,200	11,900	32,900	33,300	15.7	4.6	20.9	4.5		
15	2/6/2019	10:00:45	49.4	78,200	11,300	33,700	33,100	15.7	4.6	20.9	4.5		
16	2/6/2019	10:09:25	40	77,400	11,300	32,900	33,000	15.8	4.5	21	4.5		
17	2/6/2019	10:17:41	35	76,800	11,100	32,900	32,800	15.8	4.6	21	4.5		
18	2/6/2019	10:25:19	43.8	76,700	11,500	31,900	33,200	15.7	4.6	21	4.5		
19	2/6/2019	10:31:47	40.6	78,000	11,700	33,900	32,500	15.8	4.5	20.9	4.5		
20	2/6/2019	10:44:26	35.6	76,900	11,300	32,800	32,800	15.8	4.6	21	4.5		
21	2/6/2019	10:52:07	48.8	78,400	11,600	32,600	34,100	15.7	4.6	20.9	4.5		
22	2/6/2019	10:59:33	44.4	74,600	11,100	31,700	31,700	15.7	4.6	21	4.5		
23	2/6/2019	11:07:26	35	76,400	11,100	32,200	33,000	15.8	4.6	21	4.5		
24	2/6/2019	11:15:47	44.4	74,800	11,100	31,900	31,700	15.8	4.5	21	4.5		
25	2/6/2019	11:23:53	40	77,600	10,900	33,400	34,100	15.7	4.5	20.9	4.4		
26	2/6/2019	11:31:33	54.4	76,900	11,300	32,400	33,300	15.8	4.5	21.2	4.5		
27	2/6/2019	11:40:56	50	77,600	11,500	31,900	34,100	15.7	4.6	20.9	4.5		
28	2/6/2019	11:48:26	54.4	75,200	11,300	31,900	32,100	15.8	4.6	20.9	4.5		
29	2/6/2019	12:04:12	53.1	78,000	11,000	33,000	34,000	15.8	4.6	21	4.5		
30	2/6/2019	12:11:18	53.8	74,700	11,200	32,100	31,200	15.8	4.6	21	4.5		

Run	DATE	TIME	SPEED	WEIGHTS (pounds)				AXLE SPACINGS (feet)			
				GVW	STEER AXLE	DRIVE AXLE	TRAILER AXLE	AXLE 1-2	AXLE 2-3	AXLE 3-4	AXLE 4-5
1	2/7/2019	8:42:16	38.8	80,534	11,200	34,590	34,744	15.6	4.45	20.65	4.4
2	2/7/2019	8:52:39	38.8	79,896	11,046	34,148	34,702	15.7	4.55	20.75	4.45
3	2/7/2019	8:58:56	41.3	79,874	10,824	32,914	36,132	15.6	4.55	20.65	4.45
4	2/7/2019	9:01:44	39.4	80,866	11,134	33,664	36,068	15.6	4.55	20.65	4.4
5	2/7/2019	9:06:22	40.6	81,042	11,860	34,216	34,964	15.7	4.55	20.85	4.45
6	2/7/2019	9:11:13	38.8	77,514	10,934	32,960	33,620	15.55	4.45	20.5	4.4
7	2/7/2019	9:19:08	44.4	78,704	10,802	33,644	34,260	15.6	4.5	20.75	4.45
8	2/7/2019	9:22:30	44.4	80,490	11,046	35,142	34,304	15.55	4.5	20.65	4.35
9	2/7/2019	9:25:56	43.8	80,712	11,090	33,886	35,736	15.6	4.5	20.65	4.45
10	2/7/2019	9:29:57	43.8	79,058	11,398	33,222	34,436	15.7	4.5	20.85	4.45
11	2/7/2019	9:33:16	43.8	76,942	10,846	32,914	33,178	15.6	4.45	20.6	4.45
12	2/7/2019	9:38:39	45	78,088	10,516	32,474	35,098	15.65	4.5	20.85	4.45
13	2/7/2019	9:41:37	48.8	78,132	10,980	33,156	33,994	15.65	4.5	20.7	4.4
14	2/7/2019	9:46:35	50	77,294	10,846	33,158	33,290	15.7	4.55	20.95	4.45
15	2/7/2019	9:51:25	47.5	78,816	10,980	33,202	34,634	15.6	4.55	20.75	4.4
16	2/7/2019	9:53:38	50.6	77,316	11,112	33,136	33,068	15.7	4.5	20.85	4.45
17	2/7/2019	9:58:14	48.8	77,890	11,024	33,180	33,686	15.6	4.5	20.65	4.4
18	2/7/2019	10:00:42	49.4	77,140	11,200	32,474	33,466	15.6	4.55	20.75	4.45
19	2/7/2019	10:04:09	48.8	78,528	11,222	33,112	34,194	15.7	4.5	20.75	4.4
20	2/7/2019	10:12:17	49.4	77,734	11,354	32,760	33,622	15.75	4.55	21	4.45
21	2/7/2019	10:15:24	38.8	74,538	10,186	31,968	32,386	15.55	4.5	20.55	4.35
22	2/7/2019	10:19:28	45	75,464	11,156	32,298	32,012	15.7	4.55	20.85	4.45
23	2/7/2019	10:22:42	48.1	80,028	11,288	33,532	35,206	15.6	4.5	20.65	4.4
24	2/7/2019	10:27:52	40	78,594	11,244	34,236	33,114	15.7	4.5	20.85	4.45
25	2/7/2019	10:30:48	48.8	79,520	11,684	33,754	34,084	15.6	4.55	20.65	4.4
26	2/7/2019	10:35:35	35	78,330	10,648	34,062	33,622	15.6	4.5	20.7	4.4
27	2/7/2019	10:38:28	34.4	78,750	10,692	33,554	34,502	15.6	4.5	20.7	4.35
28	2/7/2019	10:43:23	49.4	78,704	11,574	32,606	34,524	15.7	4.5	20.85	4.45
29	2/7/2019	10:46:51	53.1	79,940	11,574	34,810	33,554	15.7	4.5	20.75	4.4
30	2/7/2019	10:50:06	53.1	81,704	11,266	33,774	36,664	15.7	4.5	20.85	4.45
31	2/7/2019	10:53:33	57.5	76,214	10,802	32,606	32,804	15.6	4.5	20.7	4.45

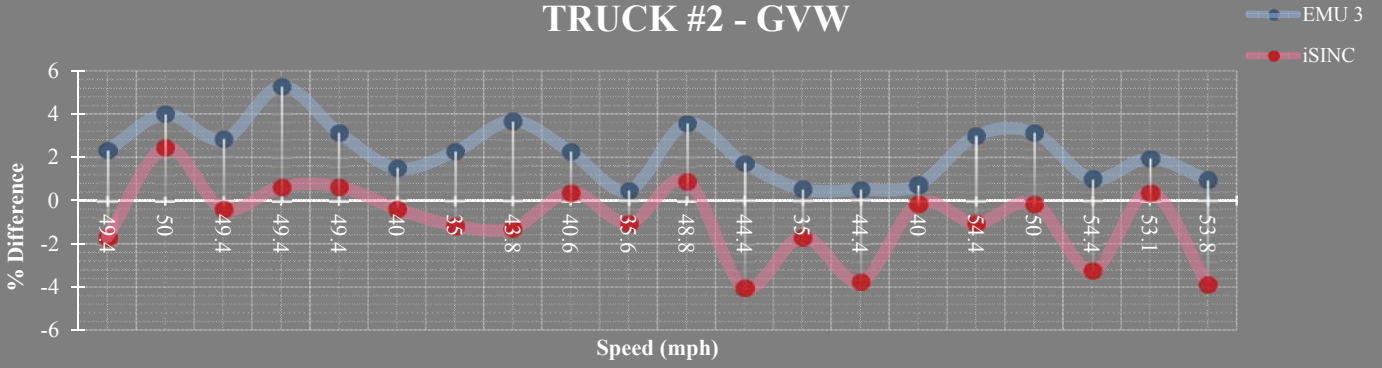
Run	DATE	TIME	SPEED	WEIGHTS (pounds)				AXLE SPACINGS (feet)			
				GVW	STEER AXLE	DRIVE AXLE	TRAILER AXLE	AXLE 1-2	AXLE 2-3	AXLE 3-4	AXLE 4-5
1	2/7/2019	8:42:16	38.8	79,000	11,100	33,500	34,500	15.6	4.5	20.7	4.4
2	2/7/2019	8:52:39	38.8	80,200	11,100	34,100	34,900	15.7	4.5	20.7	4.5
3	2/7/2019	8:58:56	41.3	80,200	10,900	33,200	36,100	15.6	4.5	20.6	4.4
4	2/7/2019	9:01:44	39.4	79,500	10,800	33,300	35,400	15.6	4.6	20.6	4.5
5	2/7/2019	9:06:22	40.6	80,000	11,200	33,400	35,400	15.7	4.5	20.7	4.4
6	2/7/2019	9:11:13	38.8	79,000	10,900	33,400	34,900	15.7	4.5	20.7	4.4
7	2/7/2019	9:19:08	44.4	76,100	10,500	31,900	33,600	15.5	4.5	20.8	4.5
8	2/7/2019	9:22:30	44.4	76,300	10,500	32,900	32,900	15.5	4.5	20.7	4.4
9	2/7/2019	9:25:56	43.8	78,500	10,500	32,800	35,100	15.6	4.6	20.8	4.5
10	2/7/2019	9:29:57	43.8	79,200	10,900	33,100	35,200	15.7	4.6	20.7	4.4
11	2/7/2019	9:33:16	43.8	77,400	10,500	33,100	33,900	15.5	4.5	20.8	4.4
12	2/7/2019	9:38:39	45	77,800	11,000	32,300	34,600	15.7	4.5	20.8	4.5
13	2/7/2019	9:41:37	48.8	78,300	10,700	33,100	34,700	15.6	4.6	20.7	4.4
14	2/7/2019	9:46:35	50	75,200	10,400	32,100	32,600	15.6	4.5	20.8	4.5
15	2/7/2019	9:51:25	47.5	78,400	11,200	33,000	34,200	15.6	4.6	20.7	4.4
16	2/7/2019	9:53:38	50.6	76,100	10,900	31,900	33,400	15.7	4.5	20.7	4.4
17	2/7/2019	9:58:14	48.8	76,800	10,900	33,200	32,800	15.6	4.5	20.7	4.4
18	2/7/2019	10:00:42	49.4	76,900	11,100	32,500	33,300	15.7	4.5	20.8	4.5
19	2/7/2019	10:04:09	48.8	78,100	10,600	33,700	33,700	15.7	4.5	20.7	4.4
20	2/7/2019	10:12:17	49.4	76,100	11,300	31,700	33,000	15.7	4.5	20.7	4.4
21	2/7/2019	10:15:24	38.8	79,000	10,700	32,900	35,200	15.6	4.5	20.7	4.4
22	2/7/2019	10:19:28	45	73,400	10,800	31,300	31,500	15.7	4.5	20.7	4.4
23	2/7/2019	10:22:42	48.1	78,600	10,500	33,200	34,800	15.6	4.5	20.7	4.5
24	2/7/2019	10:27:52	40	81,000	11,100	34,600	33,800	15.6	4.5	20.7	4.4
25	2/7/2019	10:30:48	48.8	78,500	11,000	33,600	33,900	15.6	4.5	20.8	4.5
26	2/7/2019	10:35:35	35	79,400	10,500	33,600	35,300	15.7	4.5	20.7	4.4
27	2/7/2019	10:38:28	34.4	79,200	10,700	33,600	34,900	15.6	4.5	20.8	4.4
28	2/7/2019	10:43:23	49.4	77,200	10,900	32,200	34,100	15.7	4.5	20.7	4.4
29	2/7/2019	10:46:51	53.1	80,600	11,200	34,200	35,400	15.6	4.6	20.7	4.4
30	2/7/2019	10:50:06	53.1	80,100	11,400	33,800	34,900	15.7	4.5	20.7	4.5
31	2/7/2019	10:53:33	57.5	79,500	11,500	33,700	34,300	15.7	4.6	20.8	4.4

APPENDIX C – Individual Truck Plots Vs. Speed (Phase 1)

TRUCK #1 - GVW



TRUCK #2 - GVW



APPENDIX D – Decision Trees

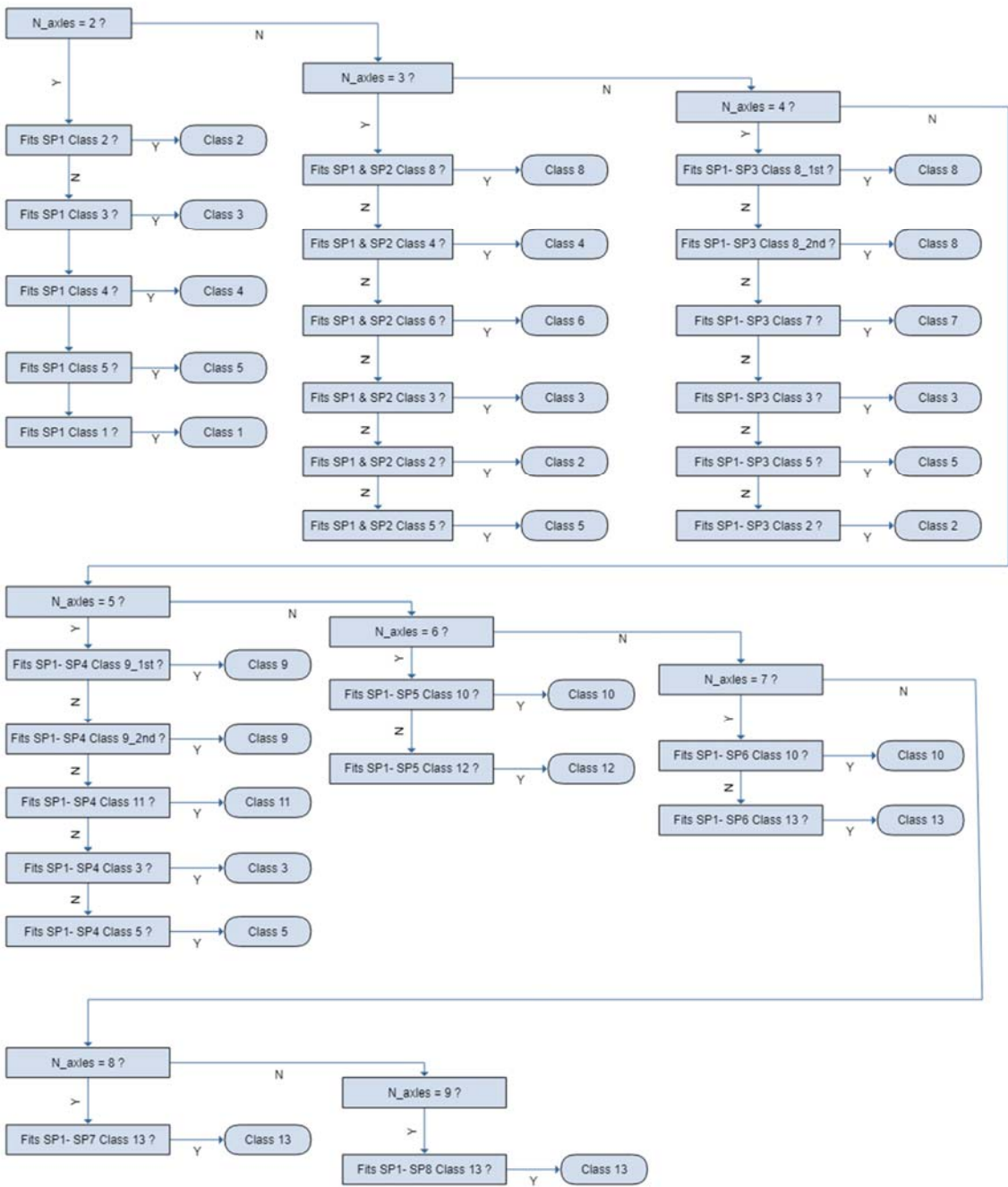


FIGURE D1: Decision Tree Used by Q-Free/TDC on EMU3

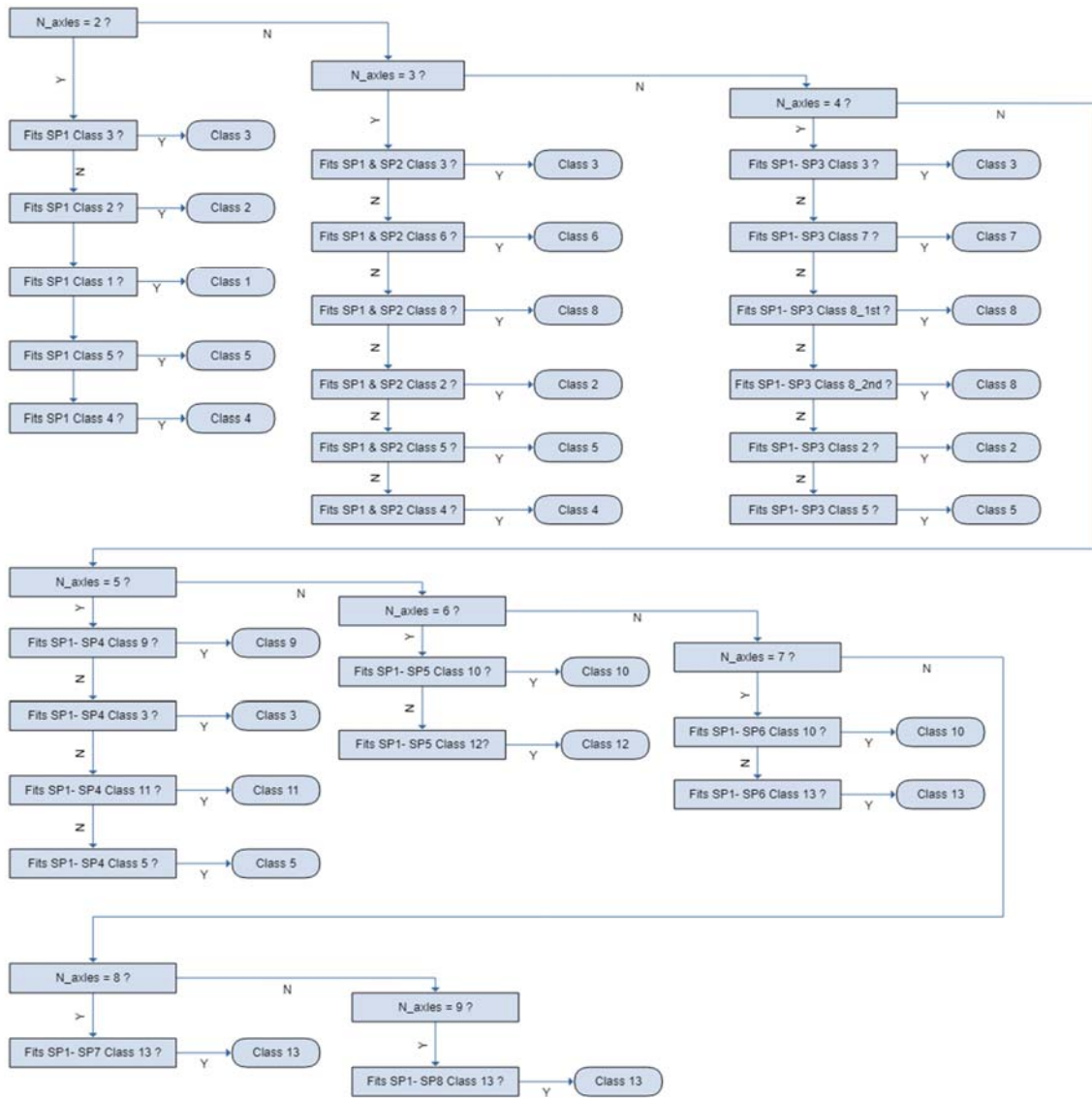


FIGURE D2. Decision Tree Used by Peek Traffic on ADR 3000

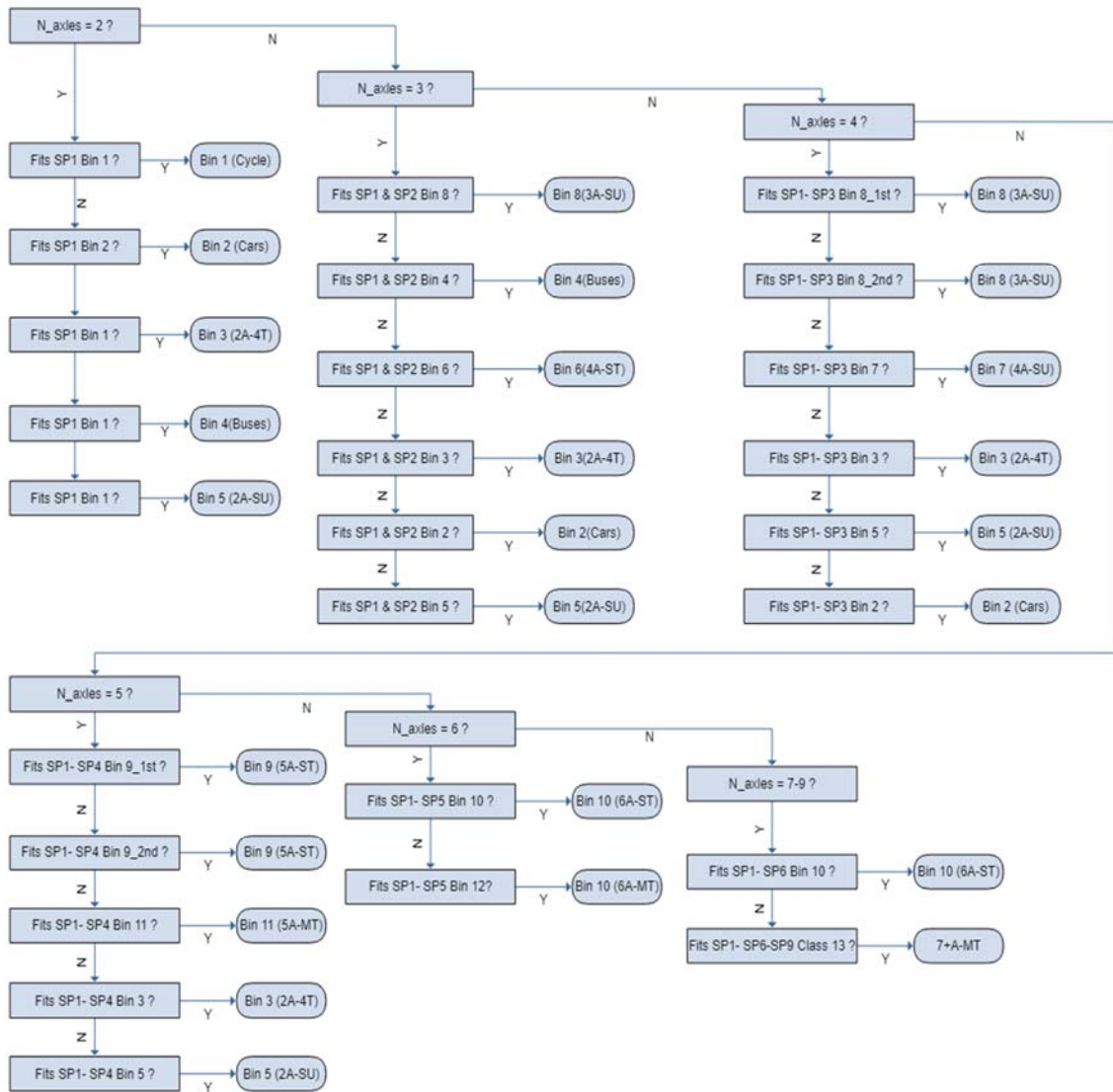


FIGURE D3: Decision Tree Used by Diamond Traffic on Phoenix 2

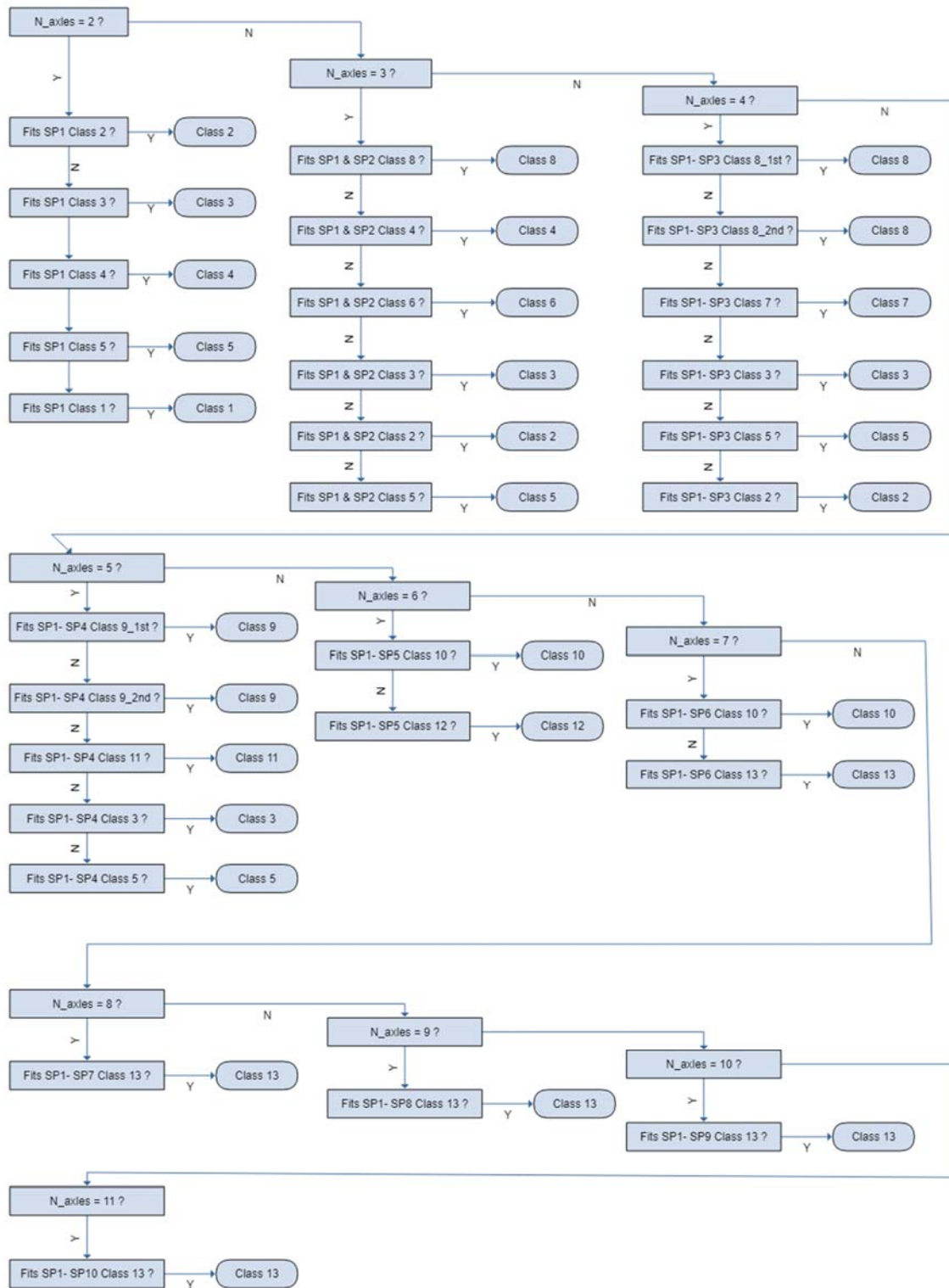


FIGURE D4: Decision Tree Used by IRD on iSINC

APPENDIX E – Equipment Certification Form

Test Date:		Test Begin Time: AM / PM		Test End Time: AM / PM	
Test Site Location:		Traffic Monitoring Equipment Being Tested			
		Make:			
Test Site Direction:		Model No.:		Serial No.	
COMPARATIVE ANALYSIS					
Results of Equipment Tested			Continuous or Visual Test Results		
Total Vehicles Counted:			Total Vehicles Counted:		
Vehicle Counts (By Class) If Applicable:			Vehicle Counts (By Class) If Applicable:		
Class 1:			Class 1:		
Class 2:		Class 1-3	Class 2:		Class 1-3
Class 3:			Class 3:		
Class 4:			Class 4:		
Class 5:			Class 5:		
Class 6:		Class 4-8	Class 6:		Class 4-8
Class 7:			Class 7:		
Class 8:			Class 8:		
Class 9:			Class 9:		
Class 10:			Class 10:		
Class 11:		Class 9-13	Class 11:		Class 9-13
Class 12:			Class 12:		
Class 13:			Class 13:		
Class 15:		Class 15	Class 15:		Class 15
Total:			Total:		
This is to certify that the portable traffic monitoring equipment listed above was tested in accordance with the guideline on the reverse of this form (to be incorporated in a procedure currently being developed), and meets the accuracy requirements needed for traffic data programs. Otherwise, the equipment is "REJECTED" as reflected in the comments section below.					
Test Performed By:					
Name		Title			
Organization		Signature			
Test Monitored / Analyzed By:					
Name		Title			
Organization		Signature			
Comments		REJECTED WHEN THIS BOX IS CHECKED		<input type="checkbox"/>	

FIGURE E1: Traffic Monitoring Equipment Certification Form (TMH, Fig 61)

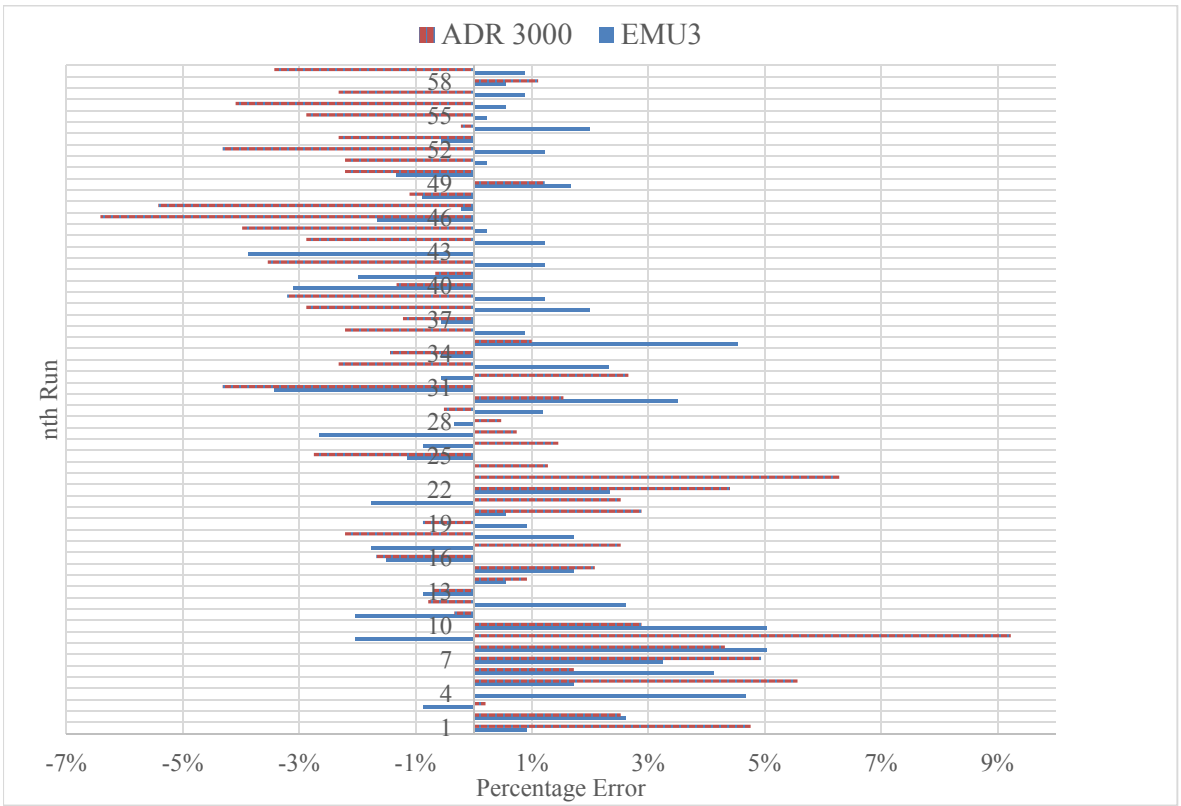


FIGURE E2: Percentage Error Distribution (Combined data)

APPENDIX F – RidePod BT Bike Tube Counter by *MetroCount*



RidePod® BT Bike Tube Counter

Optimised For Bicycle Detection

The RidePod® BT use the core technology of the RidePod VT, but has been adapted to monitoring on dedicated bike paths and on-road bike lanes. With thin-walled pneumatic tubes and overall increased sensor sensitivity (assuring bike axles are detected) and MTE's proprietary algorithms, the RidePod BT achieves unmatched accuracy in bike data interpretation.

Store 4 Million Axles

Improved memory capacity enables the RidePod BT to store up to 1 million bikes, allowing longer traffic studies. In low traffic conditions, the RidePod BT can be used for semi-permanent applications.

Up To 4 Years Battery Life

The RidePod BT will record bikes for around 4 years without a battery change. Alkaline battery packs are easily user replaceable. Remaining battery life is projected in the MTE® software to ensure that necessary changes can be made pre-survey.

Recording capacity

Bicycle volume / day	Capacity (days)
16,000	120
8,000	240
4,000	480
2,000	960

Remote Access with FieldPod®

RidePod® + FieldPod®

The RidePod BT can be amplified by the FieldPod remote access add-on. Through the mobile network, FieldPod enables data download, sensor checks and site diagnostics. Subscribers can also choose to receive customised reports regularly.

Combining RoadPod BT with FieldPod provides access to the latest data at the click of a button.

Additional hardware is required to enable FieldPod, including a remote access module, an antenna and extra battery.

MetroCount offers enclosure options and supplies components for customised solutions.

Enclosure Options



The RidePod® BT can be extended with FieldPod® remote access in a range of customisable enclosures like the pictured Pelican case.





Installation of RidePod® BT is simple and quick.



RidePod® BT recording bikes on a dedicated bike path.



RidePod® BT 5926 Hardware Specifications

Sensor type: Thin-walled, pneumatic tubes

Memory: Up to 4 million axles

Memory type: Flash

Internal battery: 6V 18Ah, 4 D alkaline cell

Time resolution: Better than 0.688ms

Enclosure: Dual system with stainless steel road case and internal unit

Dimensions: Stainless steel road case – 350mm x 124mm x 95mm

Total weight: ~4.13kg

Included: MTE® v5.x software

Required accessories: Traffic survey field kit, data communications cable

Add-ons: Remote Access Module

Australia

+61 8 9430 6164
sales@metrocount.com

Europe

+44 20 8782 8999
uksales@metrocount.com

America

+1 301 497 6101
usasales@metrocount.com

APPENDIX G – HI-TRAC OH-PED by *Q-Free*

PRODUCT SHEET

HI-TRAC® OH-PED

OVERHEAD PEDESTRIAN MONITORING UNIT

- High-accuracy overhead pedestrian detection
- Directional monitoring
- Integrates with the HI-TRAC® EMU3 and HI-TRAC® CMU traffic and bicycle counters
- Distinguishes pedestrians from other traffic



OVERVIEW

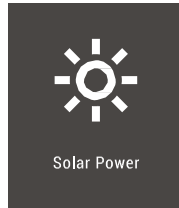
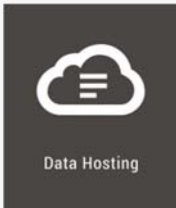
The HI-TRAC® OH-PED Overhead Pedestrian Sensor is flexible, accurate, easy to install and can be configured for a wide range of monitoring situations. It's available with two coverage patterns dependent upon mounting height and detection area required.

It functions optically, seeing the heat emitted by people passing underneath as infrared radiation through a germanium lens with a 60° field of view. The sensing area is a square on the ground whose width is approximately equal to the mounting height.

The HI-TRAC® OH-PED sensor connects to the HI-TRAC® CMU Cycle Counter or the HI-TRAC® EMU3 Traffic & Cycle Counter providing directional, zonal pedestrian detection.

The CMU & EMU3 combine the pedestrian data with that collected by other traffic sensors to accurately determine the breakdown of pedestrians and other traffic in the detection zone.

KEY FEATURES



LEADING THE WAY

PRODUCT SHEET

ADDITIONAL FEATURES

- Integrates with Q-Free's HI-TRAC® EMU3 and HI-TRAC® CMU
- Operates in all weather conditions
- User-definable count lines
- Operation independent of ambient light
- Multi-directional counting

TECHNICAL SPECIFICATIONS

COVERAGE PATTERN

	Height (m)	Min Coverage (m)
60° (PED60)	2.2–4.8	1.78–4.33
40° (PED40)	4.0–7.5	2.16–4.34

Note: The mounting height determines the maximum coverage area available as shown above.

Detection Speed Range: 0.5ms⁻¹ – 3ms⁻¹

Count lines and registers can be configured to count in both directions. The lines can be user-configured in a number of ways:

COUNT DIRECTION

People are counted when they cross the count lines. Different 'count modes' are available. The direction of line crossing which increments the count is user-selectable and is indicated by the arrows on the counting lines.

COUNT MODES

Various count modes are available, including:

- Count increments when person crosses line
- Count increments when person leaves the field of view
- Ignore or register U-turns
- Count every line crossing or only the first line crossing

ADVANCED COUNT LINES LOGIC

Embedded within the overhead pedestrian sensor is the ability to use multiple count lines to extract more detailed information about people's movements within the field of view of the counter. Using logic such as

Sequential, Summation and Alternative it is possible to get advanced analytical information for a variety of applications. For example, by using sequential line logic a new register can be created that will only increment when a person crosses two count lines in a predetermined order. Such an application is useful in determining the flow of people in different directions from an entrance.

MECHANICAL, WEIGHTS & DIMENSIONS

Housing	Die-cast aluminium
Coating	Grey Powder Coat (RAL 7001)
Dimensions	140 x 133 x 80mm (60° & 40° lenses)
	140 x 133 x 88mm (20° lens)
Weight	<500g
Mounting	Four fixing holes in base or mountable using accessory ball joint mounting

The front part of the unit is removable from the base in a 'twist and pull' action.

POWER SUPPLY

Supply voltage	12–28 VDC
Ripple	< 2Vpk-pk within supply voltage
range Typical Supply Current	100mA at 12V

INSTALLATION

- Minimal set-up and installation required
- Installs directly above detection zone

70mA at 24V

Adverse thermal environments: Areas of intense sunlight with localised temperature variations and rapid changes in temperature may adversely affect performance of the counter.

www.q-free.com

For more information contact marketing@q-free.com

S
p
e
c
i
f
i
c
a
t
i
o
n
s
a
r
e
s
u
b
j
e
c
t
t
o
c
h
a
n
g
e
w
i
t
h
o
u
t
p
r
i
o
r
n
o
t
i
c
e
.
C
o
p
y

APPENDIX H – Urban Post MULTI by *Eco-Counter*

Overview

The **Urban Post** is a highly accurate and **robust** person counting system. The Urban Post counts both cyclists and pedestrians and is ideal as a permanent counter in parks and along paved trails. Using a PYRO sensor with its **passive-infrared, pyroelectric technology** and a **high-precision lens**, the **Urban Post** counts people passing within the range of the sensor by detecting their body temperature.

Due to its well-engineered **sensor and innovative ORION algorithm**, the Urban Post outdoor people counter **can simultaneously detect two people walking in a slightly staggered formation**. The post can be easily installed on any existing hard surface and the sensor is self-calibrating making for a simple installation.



Measure Pedestrian and Cyclist Volumes

The **Urban Post** is a multi-purpose pedestrian traffic counter and bike counter system. It is a perfect solution for counting pedestrians and cyclists on multi-user paths. The sensor monitors both pedestrians and cyclists by measuring the heat emitted by the user. The system maintains a high level of accuracy when counting cyclists travelling at high speeds.

Turn-key Solution

Thanks to its unique design, the **Urban Post** can house the complete counting system (logger, sensor and battery) in its galvanized steel housing. The housing is vandal proof and the components are completely waterproof. The system has a **two-year battery life** when equipped with an active **automatic data transmission option (3G/GSM)** and a **ten-year battery life** with manual Bluetooth data transmission.

Capture Trends Over Time

The Urban Post is a **perfect solution for capturing trends over time**. Like all Eco-Counters, the system collects data in 15-minute or 1-hour intervals, 24/7. The data generated by the system allows for the **comparison of pedestrian and bike trips over consecutive months**,

seasons or even years.

Specifications

Dimensions h 110 cm (3'3"), Ø12,5 cm (5.5in)

Weight 9kg (20lb) (including components)

Operating temperature -40 °C/ +50 °C (-40°F to 120°F)

Waterproof IP 66

Material Aluminium et PVC

Color grey (others may be available on request)

Range Up to 30m (98')

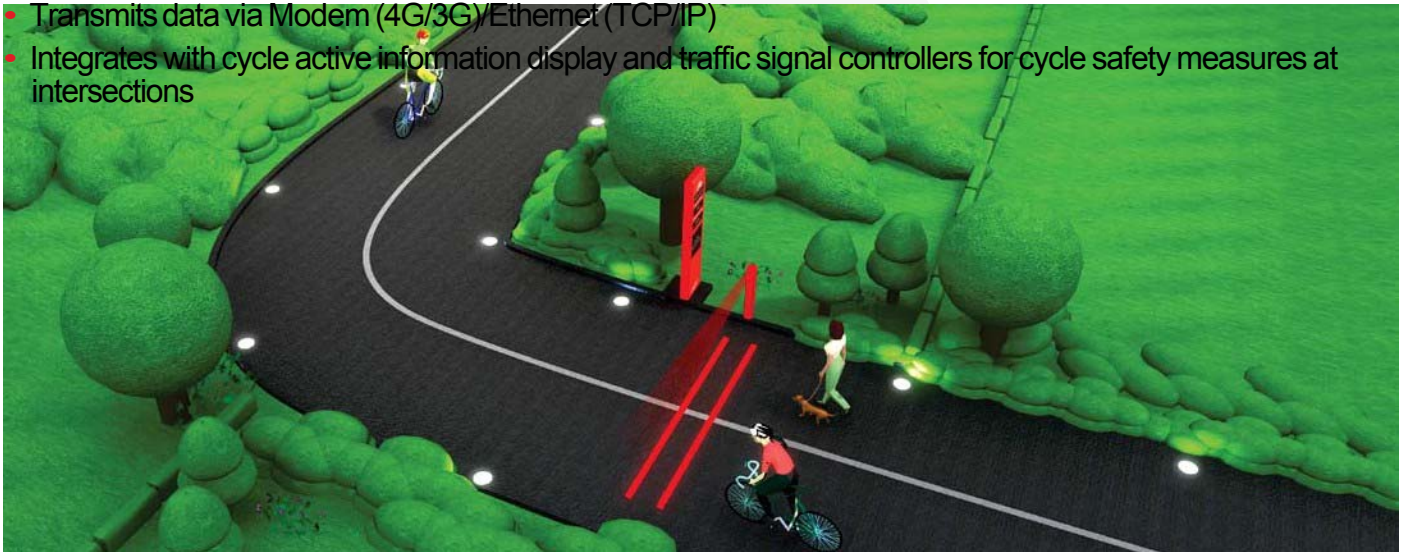
APPENDIX I – HI-TRAC CMU by *Q-Free*

PRODUCT SHEET

HI-TRAC[®] CMU

CYCLE & PEDESTRIAN MONITORING UNIT

- Simultaneously monitors cyclists and pedestrians
- Transmits data via Modem (4G/3G)/Ethernet (TCP/IP)
- Integrates with cycle active information display and traffic signal controllers for cycle safety measures at intersections



OVERVIEW

The HI-TRAC[®] CMU is a small, low-powered, low-cost electronic system capable of monitoring up to four cycle lanes and four pedestrian lanes. The CMU uses established piezo-electric sensor technology to detect bicycles in either dedicated cycle ways or mixed traffic lanes, as well as pyroelectric infrared sensors to detect pedestrians. The CMU also detects bicycles constructed of non-metal material such as carbon fibre - a major advantage to loop based technologies.

Highly accurate pedestrian detection is available via the integration of passive infrared sensor mounted on the roadside pillar or for improved accuracy an overhead sensor option can be provided.

Unique algorithms developed by Q-Free measure axle count, speed and wheelbase to distinguish true bicycles from other traffic including children's scooters, prams, trolleys, motorbikes and mopeds.

The CMU can be powered from as little as a small 3W solar panel mounted on top of a small pillar, supported by two rechargeable 6V 8Ah batteries to form a fully standalone permanent solution. The CMU unit is sealed to IP68 and can be installed into a small pillar or post.

It can be configured to automatically transmit traffic data via GPRS/2G/3G/4G to a web server for secure storage.

Legacy GSM dial-up communication is also supported along with local download to PC or tablet using Q-Free's HICOMM APP.



PRODUCT SHEET

KEY FEATURES

ADDITIONAL FEATURES

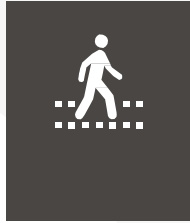
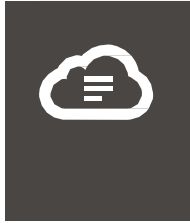
- Detects single bicycles, bicycle clusters, bicycles travelling in two directions, bicycles with pedestrians walking nearby and bicycles made of non-metals including carbon fibre - a major advantage over inductive loop based alternatives
- Measures speed, direction and gap/headway
- Vehicle-by-Vehicle (VBV) data storage
- Can be integrated with Q-Free's Cycle Information Display
- Provides triggers for cycle signal priority at traffic signalised junctions and for roadside advanced warning signs
- Can be installed into dedicated cycle ways or mixed traffic lanes
- GPRS/GSM telemetry option
- Bluetooth™ communications option
- Accurate pedestrian detection using Q-Free's recently improved pyroelectric infrared sensors
- Offers Modem (3G/4G) or Ethernet (TCP/IP) as standard communication module

INSTALLATION

- Two piezo-electric sensors per cycle lane or mixed traffic lane
- One pyroelectric infrared sensor or above ground pedestrian sensor per walkway
- CMU electronics housed in above-ground pillar or cabinet
- Typical installation time of two hours

SOFTWARE

- HI-COMM 100-compatible
- Data download, analysis, real-time VBV view, report generation and diagnostics
- Data hosting and reporting service
- Android App for Bluetooth easy set-up and data retrieval



TECHNICAL SPECIFICATIONS

STORAGE CAPACITY

8GB microSD non-volatile 365-day VBV capacity

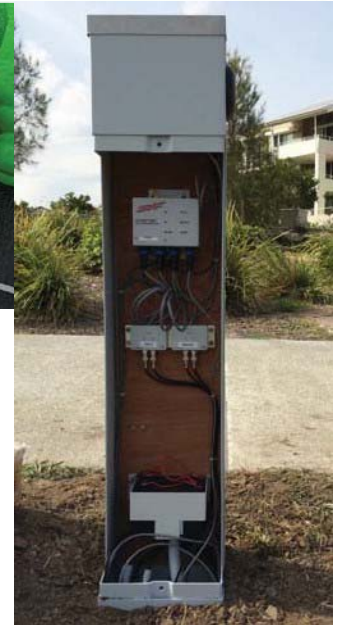
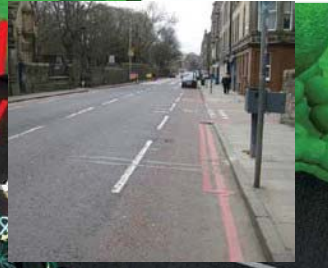
INPUT/OUTPUT PORTS

DIMENSIONS & WEIGHT

120 x 60 x 110mm (W x D x H)

Weight: 1kg

POWER SUPPLY



www.q-free.com

For more information contact marketing@q-free.com

Specifications are subject to change without prior notice.
Copyright © Q-Free 2018. All rights reserved.



APPENDIX J – Snapshot of Video Data

Hour	Minute	Time at MetroCount Second	Time at HI-TRAC Overhead Second	Time at Eco- Counter Second	Time at HI- TRAC CMU Second	Direction of Travel	Class
8	1			3	4	Eastbound	Pedestrian
8	1			14	12	Westbound	Pedestrian
8	1		53			Eastbound	Pedestrian
8	1		55			Westbound	Pedestrian
8	1		55			Westbound	Pedestrian
8	2			18	20	Eastbound	Pedestrian
8	2		27	54	55	Eastbound	Pedestrian
8	2		41			Eastbound	Pedestrian
8	2		41			Eastbound	Pedestrian
8	2			43	41	Westbound	Pedestrian
8	3		8			Westbound	Pedestrian
8	3	10	11	22	23	Eastbound	Bicyclist
8	3	20	21	32	33	Eastbound	Bicyclist
8	3					Eastbound	Pedestrian
8	3		21	24	23	Westbound	Pedestrian
8	3			31	33	Eastbound	Pedestrian
8	3			31	33	Eastbound	Pedestrian
8	3			48	47	Westbound	Bicyclist
8	3			49	50	Eastbound	Pedestrian
8	3		51			Westbound	Pedestrian
8	3			55	54	Westbound	Bicyclist
8	3			58	56	Westbound	Pedestrian
8	3			58	56	Westbound	Pedestrian
8	4			4	3	Westbound	Pedestrian
8	4	9	8			Westbound	Bicyclist
8	4	13	12			Westbound	Bicyclist
8	4		21			Eastbound	Pedestrian
8	4		33			Westbound	Pedestrian
8	4		33			Westbound	Pedestrian
8	4		33			Westbound	Pedestrian
8	4	37	38	52	53	Eastbound	Bicyclist
8	4	39	40	54	55	Eastbound	Bicyclist
8	4			44	45	Eastbound	Pedestrian
8	4			54	53	Westbound	Pedestrian
8	4		58			Eastbound	Pedestrian
8	4		58			Eastbound	Pedestrian
8	5		11			Eastbound	Pedestrian
8	5			20	19	Westbound	Bicyclist
8	5			20	19	Westbound	Pedestrian
8	5			31	33	Eastbound	Pedestrian
8	5			32	34	Eastbound	Pedestrian
8	5	49	48	33	32	Westbound	Bicyclist